https://doi.org/10.5194/egusphere-2026-2654
Preprint. Discussion started: 20 May 2026

Recent Modelling Studies Systematically Underestimate the Warming from IMO2020 Shipping Regulations

Josh Smith[1], Matthew Henry[1], Masaru Yoshioka[2], Ben Johnson[3], and Jim Haywood[1]

[1]Department of Mathematics, University of Exeter, Exeter, UK
[2]School of Earth and Environment, University of Leeds, Leeds, UK
[3]Met Office Hadley Centre, Exeter, UK

Correspondence to: Josh Smith (jgms202@exeter.ac.uk)

Abstract. The 2020 International Maritime Organisation regulations (IMO2020) reduced shipping SO_2 emissions by roughly 80 %, decreasing the cooling effect of sulphate aerosols on marine clouds, leading to a positive radiative forcing. Recent Global Climate Model (GCM) studies agree on a positive Effective Radiative Forcing (ERF) of $\sim 0.10\,\mathrm{W\,m^{-2}}$ from IMO2020. However, these studies rely on parameterisations for sub-grid scale emission processes with assumptions on primary sulphate fraction, particle size, and injection altitude, which contradict observational evidence for shipping exhaust plumes. Using the UKESM1.1 climate model, we conduct sensitivity experiments to quantify the impact of these uncertainties. We find that re-allocating primary sulphate from the accumulation and coarse modes to the Aitken mode increases the IMO2020 ERF from $0.10\,\mathrm{W\,m^{-2}}$ to between 0.19 and $0.31\,\mathrm{W\,m^{-2}}$, and additionally increasing primary sulphate fraction increases this further up to $0.41\,\mathrm{W\,m^{-2}}$. This sensitivity is driven primarily by the cloud radiative effect (ΔCRE) responding to an order-of-magnitude increase in modelled aerosol number emissions for the same sulphur mass, and is consistent with earlier shipping studies using other GCMs. Because recent GCM estimates rely on the same biased sub-grid emission assumptions, we argue this underestimate is structural across recent studies, and we find that the default-parameter experiment with a $0.10\,\mathrm{W\,m^{-2}}$ forcing significantly underestimates regional ΔCRE values relative to published satellite observations. An IMO2020 ERF 2 to 4 times the current consensus would explain a larger portion of Earth's energy imbalance since 2020 and of the recent global temperature surge.

1 Introduction

Before 2020, most commercial ships burned high sulphur heavy fuel oils (Mueller et al., 2023). Combustion of these fuels emits both sulphate aerosol (SO_4) and sulphur dioxide gas (SO_2); once emitted, SO_2 is rapidly oxidised through gas-phase and aqueous-phase pathways further contributing to sulphate aerosol mass and number. Sulphate aerosol is reflective and hygroscopic, directly reflecting additional solar radiation and increasing cloud albedo by enhancing cloud droplet number concentration (N_d) (Twomey, 1974, 1977). Additional cloud adjustments, such as precipitation suppression, extended cloud lifetime and increased cloud fraction can enhance this effect (Albrecht, 1989; Chen et al., 2022), although enhanced cloud-top entrainment and evaporation may partly offset it (Ackerman et al., 2004; Bretherton et al., 2007; Small et al., 2009).

https://doi.org/10.5194/egusphere-2026-2654
Preprint. Discussion started: 20 May 2026

Shipping emissions have a particularly effective cooling influence because they perturb highly susceptible clouds over dark ocean surfaces (Bellouin et al., 2020).

On 1 January 2020, motivated by public-health concerns (Corbett et al., 2016), the International Maritime Organization implemented the "Marpol Annex VI" regulation (hereafter IMO2020), reducing the maximum allowable sulphur content of marine fuels from 3.5 % to 0.5 % (IMO, 2019). This cut shipping SO_x emissions by ∼80 % corresponding to a roughly 8 Tg per year reduction in major emissions inventories (Hoesly et al., 2018; Klimont et al., 2017). This has resulted in a positive radiative forcing and associated warming, resulting from an unmasking of the cooling effect of shipping SO_x emissions. (Capaldo et al., 1999; Jin et al., 2018; Lauer et al., 2007, 2009; Partanen et al., 2013; Peters et al., 2012, 2013; Righi et al., 2011; Sofiev et al., 2018).

Observations have shown both a decrease in the number of detectable ship tracks (Watson-Parris et al., 2022; Yuan et al., 2022) and large-scale regional changes to cloud microphysics from IMO2020 (Diamond, 2023; Manshausen et al., 2023). However, attributing observed global cloud and radiative perturbations to IMO2020 remains challenging due to large natural variability and a pre-existing downward trend in cloud brightness, related to broader anthropogenic aerosol emission reductions (Gettelman et al., 2024; Watson-Parris et al., 2022; Zhang et al., 2025). Consequently, Global Climate Model (GCM) experiments remain essential for quantifying the effective radiative forcing (ERF) associated with IMO2020. Due to their resolution GCMs must parameterise a range of important processes, introducing structural uncertainty. This is reflected by the spread of modelled IMO2020 forcing estimates, ranging from +0.03 to +0.33 $W\,m^{-2}$ (Bilsback et al., 2020; Partanen et al., 2013). However, more recent model experiments have converged on a tighter range of +0.07 to +0.15 $W\,m^{-2}$ (Gettelman et al., 2024; Jordan and Henry, 2024; Quaglia and Visioni, 2024; Skeie et al., 2024; Yoshioka et al., 2024; Yuan et al., 2024).

An important source of uncertainty in modelled estimates of the IMO2020 effective radiative forcing arises from the treatment of sub-grid scale emission plume processes. In GCMs, these near-source processes are necessarily represented through a small set of prescribed emission choices governing: the mass fraction of sulphur emission treated as primary sulphate aerosol at emission, the assumed particle size (modal allocation) of that primary sulphate, and the emission altitude of shipping SO_x. Available observations of ship exhaust suggest that rapid sulphate formation and emitted size distributions may not be optimally represented by default model parameters; we discuss this in detail in Sect. 2.

It has been demonstrated that the cloud radiative effect (CRE) from shipping emissions is sensitive to uncertainties in primary sulphate fraction (Partanen et al., 2013) and primary sulphate size (Righi et al., 2011; Peters et al., 2012, 2013). Changes to the indirect and direct aerosol forcing from uncertainties in SO_x emission choices for all anthropogenic sources have also been quantified across multiple models (Ahsan et al., 2023). However, no study has attempted to quantify any of these three uncertainties specifically in the context of the IMO2020 forcing. Additionally, since recent model estimates of the IMO2020 ERF rely on similar assumptions regarding the representation of these processes (Table A1) it is possible that the convergence to an estimate of ∼0.1 $W\,m^{-2}$ (Figure 1) is a result of shared structural bias rather than a physical constraint. Here we present results from a set of new UKESM1.1 atmosphere-only simulations designed to evaluate the sensitivity of the IMO2020 ERF to these uncertainties.

https://doi.org/10.5194/egusphere-2026-2654
Preprint. Discussion started: 20 May 2026

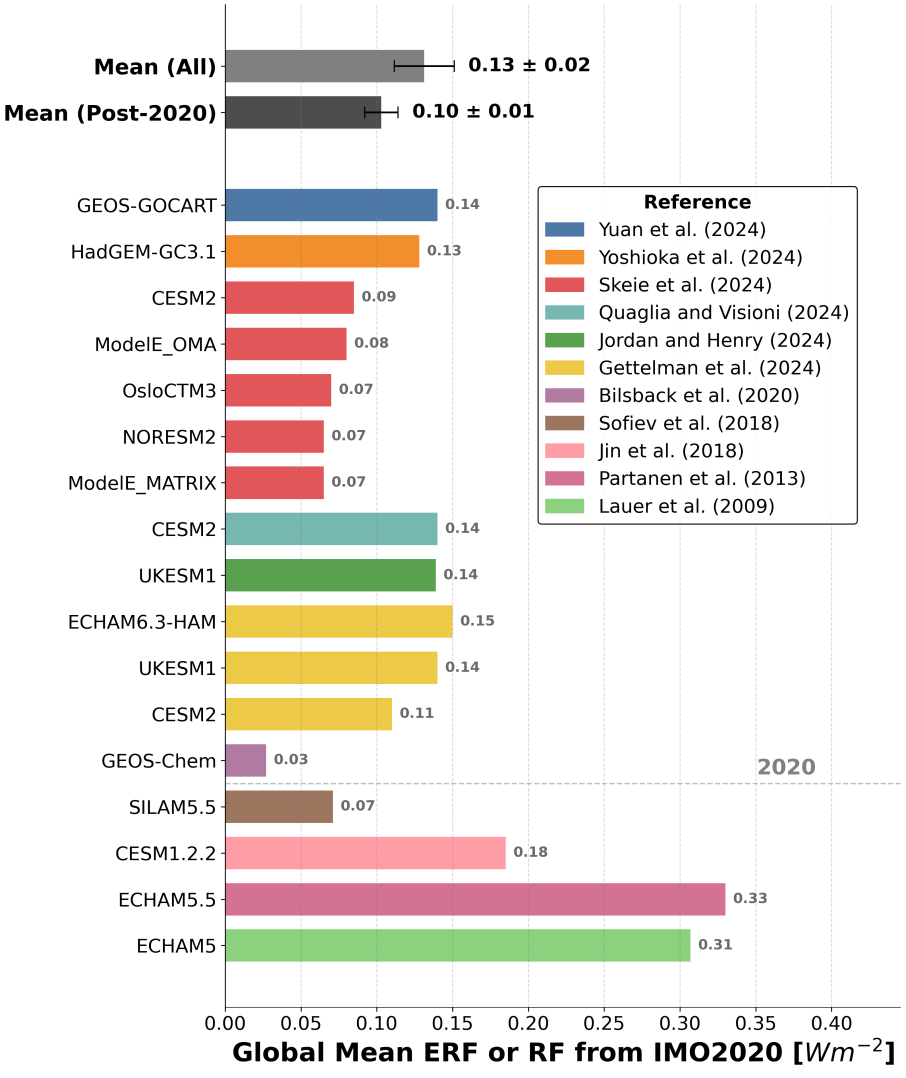

Figure 1. Effective Radiative Forcing (ERF) or Radiative Forcing (RF) estimates from all prior modelling studies. The model used is shown on the y-axis label and estimates are grouped by colour corresponding to publication. Error bars on the mean values show one standard error.

2 Model representation of near-source sulphate aerosol formation in shipping plumes

In most CMIP6-era global climate models (GCMs), including UKESM1.1, sulphur emissions are prescribed entirely as sulphur dioxide (SO_2), with a fixed fraction of emitted sulphur mass (usually 2.5 %) instantaneously converted to sulphate aerosol on emission. This primary sulphate fraction (f_{SO_4}) is set as a global constant for all natural and anthropogenic SO_x emissions, intended to parameterise rapid near-field oxidation within concentrated plumes unresolved at GCM grid scales and timesteps. This choice was made by AeroCom phase I in the early 2000s (Dentener et al., 2006; Stier et al., 2005) and has remained

https://doi.org/10.5194/egusphere-2026-2654
Preprint. Discussion started: 20 May 2026

largely unchanged since. However, since f_{SO_4} is the only source of direct sulphate aerosol emissions in GCMs, it should arguably capture sulphate aerosol formed from combustion and in exhaust systems before emission as well as unresolved sub-grid scale oxidation.

Direct measurements of ship exhaust indicate that the fraction of fuel sulphur converted to sulphate aerosol within engines and exhaust systems before emission ranges from approximately 2.4 %, at an engine load of 25 %, to 5 % at an engine load of 75 % (Agrawal et al., 2008, 2010). Typical cruising engine loads for the global fleet range from 40 to 85 % (Jalkanen et al., 2012; Borén et al., 2023). These values do not account for additional oxidation in the near-exhaust plume, where high humidity, and abundant catalysts and precursor gases promote faster sulphate nucleation than under background boundary layer conditions (Corbin et al., 2018; Ding et al., 2021; Stevens et al., 2012; Tian et al., 2014).

Aircraft measurements of ship plumes from the recent ACRUISE campaign found that SO_4 accounts for over 10 % of total S mass within 30 minutes from emission (Yu et al., 2020; Lee et al., 2025), comparable to a typical GCM time step (an atmospheric timestep in our model is 20 minutes). Furthermore, relying on a single global f_{SO_4} value fails to account for pristine marine environments, which have low condensation sinks that heavily favour rapid nucleation (Mao et al., 2021; Kerminen et al., 2018). This suggests that the commonly used 2.5 % value may represent a substantial underestimate of the effective sulphate mass fraction for shipping emissions.

In recent GCM studies, the resulting primary sulphate is typically emitted into accumulation and/or coarse aerosol modes using a uniform treatment across all anthropogenic SO_x sources. In UKESM1.1, 50 % of the primary sulphate mass is emitted into the accumulation mode and 50 % into the coarse mode following Stier et al. (2005); corresponding treatments in other GCMs used to estimate the IMO2020 forcing are summarised in Table A1 and discussed in Sect. 4.3. However, observations of ship exhaust plumes consistently show that aerosol size distributions are dominated by sulphate particles in the Aitken mode, with mean diameters (D_p) less than 90 nm (Petzold et al., 2008; Jonsson et al., 2011; Yu et al., 2020). Consistent with this, recent work has shown, using a high-resolution nested regional model, that the observed ship plume number size distributions from ACRUISE (Yu et al., 2020) cannot be reproduced without allocating all primary sulphate to Aitken mode, and either scaling f_{SO_4}, or increasing organic carbon aerosol emissions, or both (Yoshioka et al., *in prep*). The uncertainty surrounding modelled SO_x emission altitude is discussed in Methods Sect. 3.3 along with the details of our experimental design choices.

3 Methods

3.1 UKESM1.1 – general description

UKESM1.1 (Mulcahy et al., 2023) uses the HadGEM3-GC3.1 coupled climate model (Kuhlbrodt et al., 2018) as its physical core, with the Global Atmosphere 7.1 (GA7.1) atmospheric configuration (Walters et al., 2019) and atmospheric composition represented by the stratosphere–troposphere configuration of the UK Chemistry and Aerosol (UKCA) model (Archibald et al., 2020). In this study, UKESM1.1 is run in its atmosphere-only configuration, with sea surface temperatures (SSTs), sea-ice concentrations, ocean biogeochemistry, and land-surface vegetation properties prescribed using output from previous fully coupled SSP2-4.5 simulations. Aerosol number concentrations are treated prognostically using the two-moment Global Model

https://doi.org/10.5194/egusphere-2026-2654
Preprint. Discussion started: 20 May 2026

of Aerosol Processes (GLOMAP-mode) modal aerosol microphysics scheme (Mann et al., 2010, 2012) for all aerosol species except mineral dust, which is simulated using the CLASSIC dust scheme (Woodward, 2001).

For large-scale (non-convective) clouds, aerosol activation to cloud droplets is governed by the UKCA-Activate scheme (West et al., 2014), which incorporates the parameterisation of Abdul-Razzak and Ghan (2000). Large-scale cloud precipitation formation is represented by the one-moment microphysics scheme of Wilson and Ballard (1999), with autoconversion and accretion following Khairoutdinov and Kogan (2000). Large-scale cloud fraction, cloud water vapour, and liquid water content are treated prognostically using the PC2 cloud scheme (Wilson et al., 2008), with updates described by Morcrette (2012). Convective cloud processes are parameterised separately and do not explicitly account for aerosol interactions; this means that the convective cloud component of aerosol forcing is absent in UKESM1.1.

3.2 UKESM1.1 – updated configuration choices

We use an updated version of the Abdul-Razzak and Ghan (2000) (ARG2000) scheme recently developed by Ghosh et al. (2025). We chose to do this because the default ARG2000 scheme inadequately represents cloud droplet activation by over-suppressing maximum supersaturation under high aerosol low updraft conditions (Ghan et al., 2011; Nenes and Seinfeld, 2003; Phinney et al., 2003). Ghosh et al. (2025) re-tuned three parameters to better capture kinetic limitations on activation, reducing this bias and improving agreement with a cloud parcel model; we refer to the ARG scheme with these updates implemented as ARG-G25 hereafter. The largest impacts on activation from ARG-G25 occur for Aitken mode aerosols in polluted, low-updraft regimes which is potentially important for marine stratocumulus in major shipping corridors. We also implement a correction to the hygroscopicity (κ) parameter values in UKCA based on the recommendations of Petters and Kreidenweis (2007); this reduces the sulphate κ from 0.9 in the previous default set up to 0.61. All our experiments in Table 1 use identical model configurations with both changes applied. We run additional sensitivity experiments to check if these two changes impact our results (Sect. 4.1).

3.3 Experimental design

We follow the ERF diagnostic methodology of Jordan and Henry (2024), using free-running ensembles of 10-year (119 months) fixed SST simulations as recommended by Forster et al. (2016). Each experiment comprises a control (CTL) and an IMO pair (Table 1), with ensembles of 5 to 10 members per pair used to isolate the forced response from internal variability. The parameter space defined by varying primary sulphate fraction (f_{SO_4}), primary sulphate mode allocation, Aitken-mode size, and emission altitude includes substantially more combinations than could feasibly be simulated. Our experimental matrix is therefore designed to isolate the response to individual parameters, explore the combined response under physically motivated parameter sets, and allow for easier comparison to some prior studies.

https://doi.org/10.5194/egusphere-2026-2654
Preprint. Discussion started: 20 May 2026

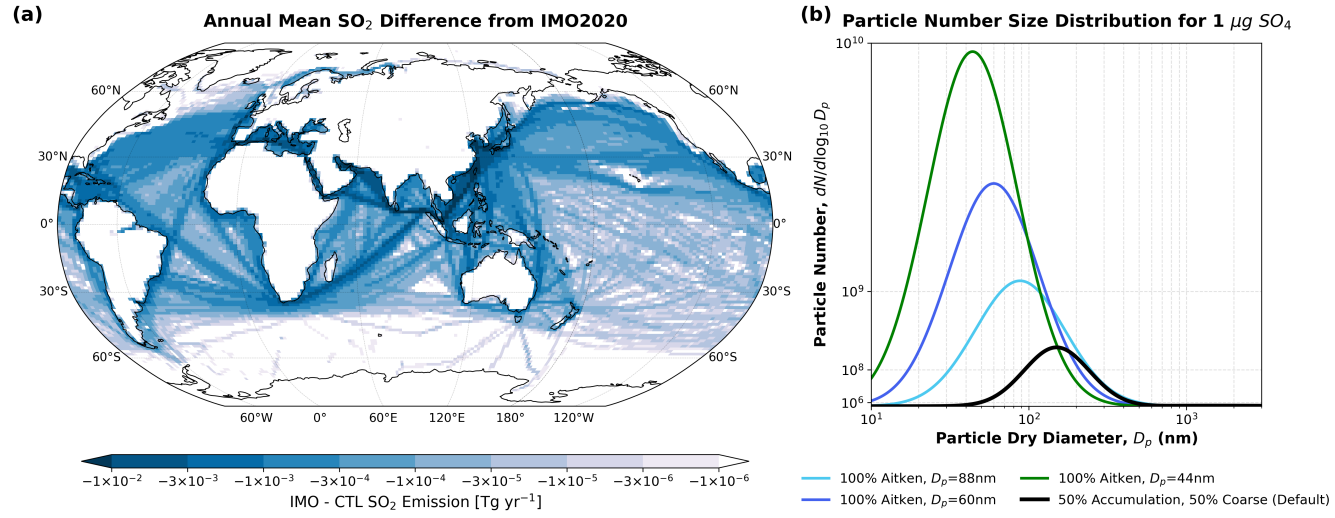

Figure 2. (a) Annual mean SO_x emission difference [Tg yr^{-1}] between our Control (CTL) and IMO experiments, averaged over our 10-year simulation duration. (b) Particle number size distribution for 1 μg SO_4 for the three different Aitken mode primary SO_4 sizes we use and the UKESM default primary SO_4 size distribution (50 % coarse with $D_p = 1500$ nm and 50 % accumulation with $D_p = 150$ nm) shown by the black line.

3.3.1 Emissions set-up

Sea ice and SST are prescribed from a 2005 to 2014 climatology following Forster et al. (2016), with other surface boundary conditions taken from the parent SSP2-4.5 simulation (Sect. 3.1). Greenhouse gas concentrations and non-shipping anthropogenic emissions follow SSP2-4.5 (O'Neill et al., 2016), with non-shipping emissions from the CMIP6 CEDS dataset (Hoesly et al., 2018; McDuffie et al., 2020). These boundary conditions and non-shipping emissions are unchanged between the CTL and IMO simulations.

Shipping SO_2 emissions are from the historical CMIP7 CEDS dataset. The CTL uses 2019 emissions repeated for the full 10-year simulation, while the IMO simulations use the 2020 to 2023 data with 2023 repeated for the remaining 6 years. This captures any impact from disruptions to global commerce caused by COVID-19, although this impact on total ship traffic has been shown to be relatively small (March et al., 2021) and is small relative to the change in SO_2 emissions resulting from IMO2020 in our dataset (Fig. S1). Our dataset gives an 8.0 Tg yr^{-1} SO_2 emission reduction between CTL and IMO simulations, corresponding to a 77 % reduction in shipping SO_2 emissions which agrees with recent best estimates. Figure 2 shows the spatial distribution of this reduction, which is identical across all our experiments.

Changes to black carbon (BC) and organic carbon (OC) aerosol from shipping may have also occurred due to IMO2020 though these are harder to quantify compared to sulphur emissions, and previous work indicates that their contributions are of second-order importance for estimating the radiative effect of shipping (Peters et al., 2012). In our simulations, shipping OC

https://doi.org/10.5194/egusphere-2026-2654
Preprint. Discussion started: 20 May 2026

aerosol emissions are prescribed from the CEDS CMIP6 SSP2-4.5 inventory and are identical in the CTL and IMO experiments, while BC aerosol from shipping is not included.

3.3.2 Sensitivity tests

Table 1. UKESM1.1 experiments. Each experiment comprises a CTL (control) and an IMO run with ensemble size given as $n_{\mathrm{CTL}} + n_{\mathrm{IMO}}$. The final column entries are the mode that the $f_{\mathrm{SO_4}}$ mass is emitted into with Acc. short for accumulation and the brackets indicating the assumed mean emission diameter for the mode.

Experiment	Ensemble size	SO_2 emission altitude (m)	$f_{\mathrm{SO_4}}$ (%)	Primary sulphate size
Base	10+10	20	2.5	50 % Acc. (D_p = 150 nm), 50 % Coarse (D_p = 1500 nm)
High	10+10	100–320	2.5	50 % Acc. (D_p = 150 nm), 50 % Coarse (D_p = 1500 nm)
High_4.5	10+10	100–320	4.5	50 % Acc. (D_p = 150 nm), 50 % Coarse (D_p = 1500 nm)
Ait	5+5	20	2.5	100 % Aitken (D_p = 60 nm)
Ait_88nm	5+5	20	2.5	100 % Aitken (D_p = 88 nm)
Ait_44nm	5+5	20	2.5	100 % Aitken (D_p = 44 nm)
Ait_High	5+5	100–320	2.5	100 % Aitken (D_p = 60 nm)
Ait_High_4.5	5+5	100–320	4.5	100 % Aitken (D_p = 60 nm)
Ait_10	10+10	20	10.0	100 % Aitken (D_p = 60 nm)

Base represents the UKESM1.1 default SO_2 emission configuration used for previous IMO2020 forcing studies with models using UKCA (Gettelman et al., 2024; Jordan and Henry, 2024; Yoshioka et al., 2024). For all experiments the changes to emission assumptions are applied only to shipping SO_x emissions. All other SO_x sources are emitted into the lowest model level and use the default primary SO_4 treatment.

High represents an increase in emission altitude following the same shipping SO_x emission altitude range as the recent emissions model intercomparison project sensitivity experiments (Ahsan et al., 2023). This corresponds to model levels 3 to 6 in UKESM1.1, with the SO_x mass in each model grid box split evenly between these 4 levels.

This represents a physically motivated improvement compared to the default (*Base*) assumption where all shipping emissions are injected at 20 m, since the ship stacks of the so-called post-Panamax global shipping fleet are 50 to 70 m tall (Chosson et al., 2008; Gan et al., 2023), and plume rise (which is not resolved by GCMs) can rapidly take exhaust plumes to 100 to 500+ m (Briggs, 1965; Chosson et al., 2008; Xu et al., 2021; Badeke et al., 2022).

For a different set of sensitivity experiments, Ahsan et al. (2023) increased primary SO_4 fraction to 7.5 % for all anthropogenic emission sources. Here, based on the evidence of rapid SO_4 formation in shipping plumes presented in Sect. 2, we use a slightly higher shipping-specific $f_{\mathrm{SO_4}}$ of 10 % in one experiment. We use a middle $f_{\mathrm{SO_4}}$ of 4.5 % primary sulphate fraction which has been widely used (Lauer et al., 2007, 2009; Peters et al., 2012, 2013; Partanen et al., 2013) and update shipping primary sulphate to be all allocated to the Aitken mode, based on the evidence in Sect. 2. In experiments *Ait_88nm* and *Ait_44nm*,

https://doi.org/10.5194/egusphere-2026-2654
Preprint. Discussion started: 20 May 2026

we also test the sensitivity to varying Aitken primary sulphate size within a range used by prior modelling studies (Lauer et al., 2009; Partanen et al., 2013). All of these details and experiment names can be seen in Table 1.

3.4 ERF decomposition

We decompose the total ERF following Ghan (2013) into three components: the instantaneous radiative forcing (IRF), corresponding to aerosol–radiation interactions (ARI); the difference in cloud radiative effect (ΔCRE), predominantly caused here by aerosol–cloud interactions (ACI); and the clear-clean radiative adjustments (clear-clean RA) associated with changes to the atmospheric state and surface albedo in the absence of aerosols and clouds.

3.5 Observational data

Top of Atmosphere Cloud Radiative Effect (CRE) data used is from the Clouds and the Earth's Radiant Energy System (CERES) Energy Balanced and Filled (EBAF) Top-of-Atmosphere (TOA) Edition 4.2 dataset (Loeb et al., 2018).

4 Results and discussion

4.1 Forcing sensitivity results

In the model default configuration (*Base*), the global-mean IMO2020 ERF is 0.10 W m^{-2} (Fig. 3). This is slightly lower than the estimates of 0.14 W m^{-2} (Jordan and Henry, 2024) and 0.13 W m^{-2} (Yoshioka et al., 2024) that used previous configurations of the Met Office atmospheric model. We attribute this difference to the κ-fix (Sect. 3.2; Table S1) which reduces sulphate activation efficiency and therefore weakens the CRE component of the IMO2020 ERF. In a separate sensitivity test isolating the role of the κ-fix (*Default* versus *Base_ARG2000* in Table S1), this adjustment decreased the ERF from 0.13 to 0.10 W m^{-2}, bringing the *Base* ERF closer to the mean of post-2020 published model experiment results (Fig. 1). We also tested the impact of updating the activation scheme from ARG2000 to ARG-G25 in isolation and found it had no statistically significant impact on the IMO2020 ERF under a wide range of emission parameterisations (Table S1, Fig. S2).

Figure 3 summarises the IMO2020 ERF across the experiment suite and decomposes the response into ΔCRE, IRF, and clear-clean RA following Ghan (2013). The IMO2020 ERF shows a high sensitivity to the changes to shipping-emission assumptions, spanning a range of 0.10–0.41 W m^{-2} across our experiments. The ERF changes between experiments are dominated by changes to ΔCRE, with IRF and clear-clean RA remaining relatively stable.

This high sensitivity of the ΔCRE term is mainly due to the sensitivity of the cloud response to aerosol number emissions in our updated experiments (Figure 4d). Changing f_{SO_4} allocation to Aitken mode in isolation increases ERF strongly (by a factor of 1.9 to 3.1), with the magnitude sensitive to the assumed Aitken mean diameter (D_p). Changing from the default coarse/accumulation mode split to Aitken mode f_{SO_4} increases sulphate aerosol number emission (for a fixed SO_2 mass) by ∼10× with D_p = 88 nm, ∼31× with D_p = 60 nm, and ∼79× with D_p = 44 nm. However there are competing effects; more numerous aerosol will lead to higher N_d and so a stronger Twomey effect but only if the aerosol is above the minimum critical

https://doi.org/10.5194/egusphere-2026-2654
Preprint. Discussion started: 20 May 2026

diameter for activation. The total ERF for *Ait_88nm* is larger than *Ait* though this is likely due to noise as there is overlap between the standard error ranges and the ΔCRE term is larger in the *Ait* experiment.

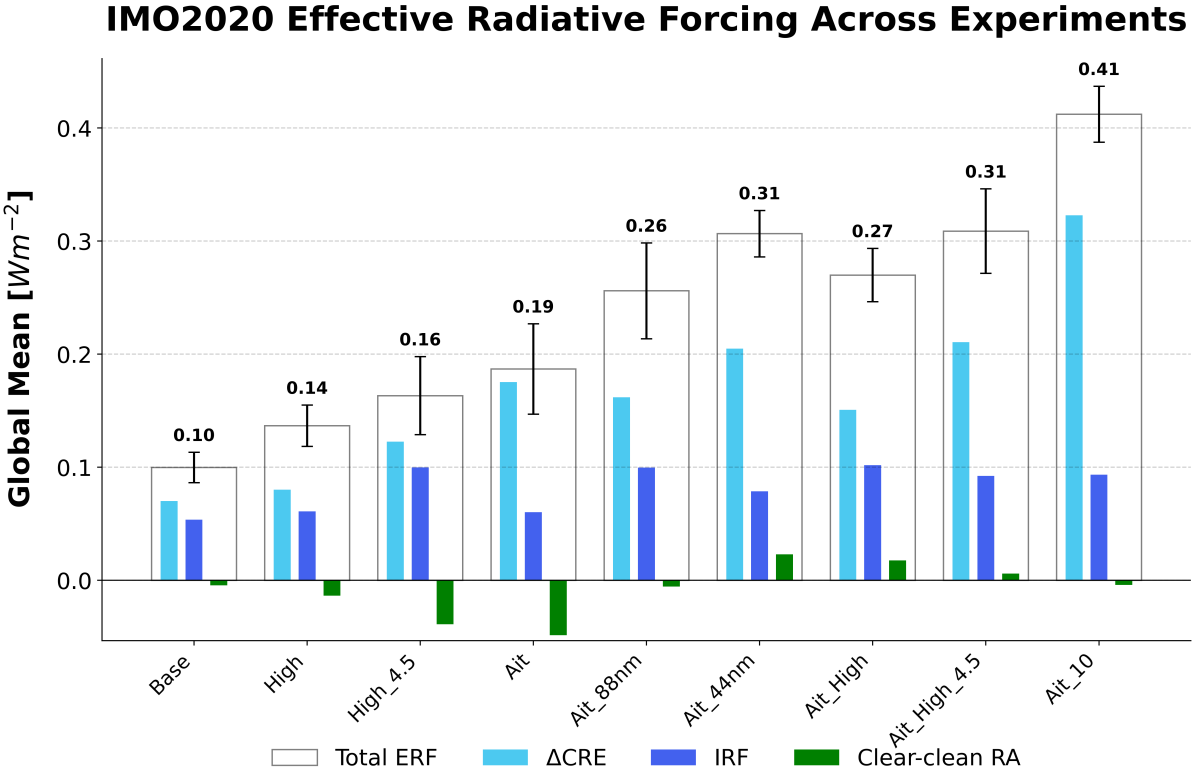

Figure 3. Ensemble mean, global mean ERF from IMO2020 and components: difference in cloud radiative effect (ΔCRE), instantaneous radiative forcing (IRF) and clear-clean radiative adjustments (clear-clean RA) calculated following Ghan (2013). Error bars are one ensemble standard error from the mean (SEM). For *Base*, *High* and *High_4.5* the Ghan decomposition quantities are computed from a subset of 7 out of the 10 ensembles members used for the ERF, all other experiments use all members for all values.

195 Increasing f_{SO_4} results in a consistent ERF increase, although the impact on the IMO2020 ERF of going from from 2.5 % to 4.5 % in isolation is not statistically significant in our results. The ERF increase from *Ait* to *Ait_10* is highly significant (p = 0.002 from a two-tailed t-test), with a factor of 4 increase in f_{SO_4} roughly doubling the IMO2020 ERF. This sensitivity also arises from the sensitivity to aerosol number since the emitted number increase from reducing primary sulphate size is being further multiplied by the f_{SO_4} scale factor.

200 We find a consistent increase in the IMO2020 ERF from increasing emission altitude, however these increases are not statistically significant in isolation, larger ensemble sizes would be needed to determine the robustness of these changes. The combined forcing impact of increasing emission altitude and reallocating f_{SO_4} to Aitken mode is slightly superadditive but is within the uncertainty range of an additive response (the ERFs of *Ait_High* - *Base* is larger than (*High* - *Base*) + (*Ait* - *Base*) but only by 0.8 times the propagated SEM).

https://doi.org/10.5194/egusphere-2026-2654
Preprint. Discussion started: 20 May 2026

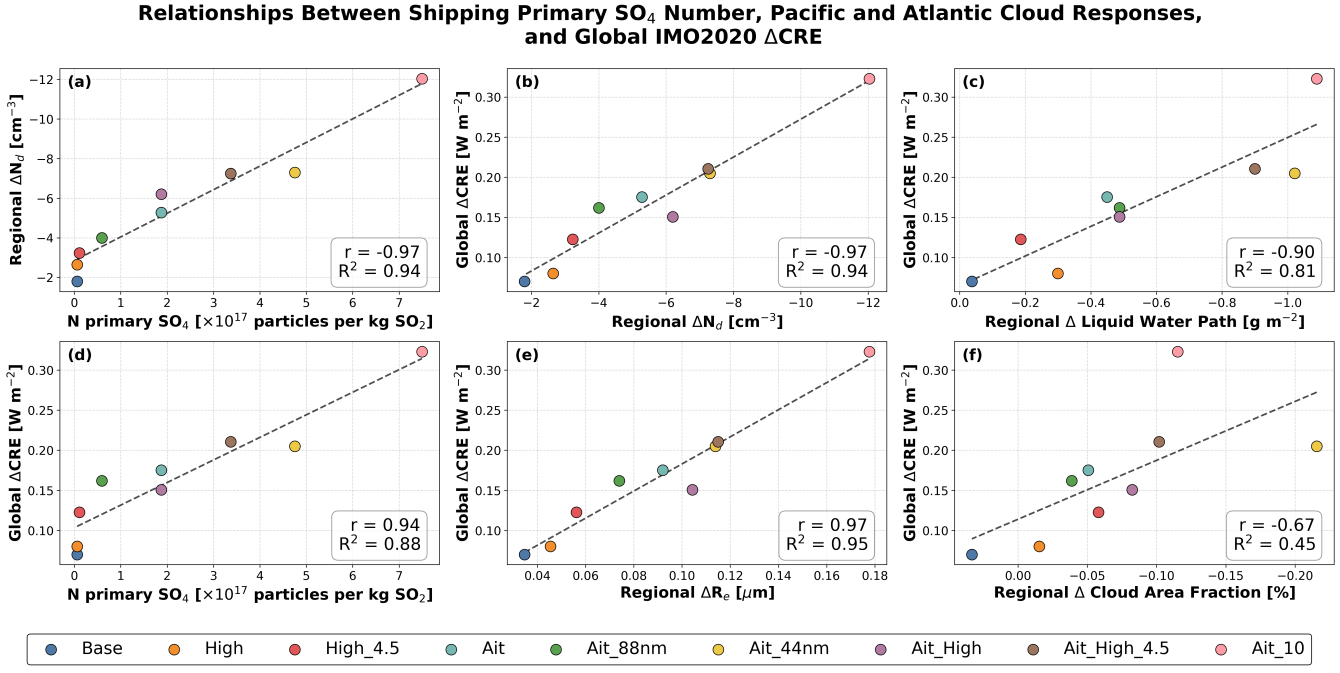

Figure 4. Relationships between the shipping primary SO_4 number per Kg of emitted SO_2, global mean ΔCRE and regional mean cloud properties calculated over the North Atlantic (20°N–70°N, 70°W–10°W), South Atlantic (SA) (65°–0°S, 25°W–15°E), and North Pacific (20°N–70°N, 140°E–120°W) in all of our experiments.

The increases in ΔCRE are spatially concentrated in regions where substantial shipping emissions are collocated with persistent low marine clouds, with the largest contributions arising from the Southeast Atlantic, North Pacific and North Atlantic (Fig. S3, S4). The global ΔCRE magnitude across experiments correlates strongly with the SO_4 aerosol number emission per unit SO_2, and the microphysical and macrophysical cloud adjustments to IMO2020 in these regions (Fig. 4). Hence the mechanism for the sensitivity we find arises from the high sensitivity to aerosol number perturbations in persistent "number-limited" marine low cloud regimes especially marine stratocumulus regions, which has been extensively documented (e.g. Twohy et al., 2005; Reutter et al., 2009; Wood, 2012; Stevens and Feingold, 2009).

4.2 Comparison to results from prior work

Lauer et al. (2007, 2009) modelled all shipping primary sulphate emissions in the Aitken mode across all experiments. The 2007 study found a larger shipping aerosol indirect effect from an inventory with a higher f_{SO_4}, although total shipping sulphur emissions were also higher in that inventory. The 2009 study estimated the IMO2020 forcing at 0.30–0.31 W m^{-2}, taken as the difference in total shipping indirect forcing between the *No Control* and *Global 0.5* experiments, with the small range coming from two different emission inventories. This is very close to the ERF estimate of 0.31 W m^{-2} from our *Ait_44nm* experiment which has the closest match to their model set up, which used $f_{SO_4} = 2.5\,\%$ in Aitken mode with $D_p = 30$ nm.

https://doi.org/10.5194/egusphere-2026-2654
Preprint. Discussion started: 20 May 2026

Righi et al. (2011) found a high sensitivity of the indirect radiative forcing from shipping to the assumed size of primary sulphate aerosol emissions; the total indirect forcing from shipping was $-0.4\,\mathrm{W\,m^{-2}}$ for their experiment with all primary sulphate in Aitken mode with $D_p = 30\,\mathrm{nm}$ and $f_{\mathrm{SO_4}} = 2.5\,\%$.

Peters et al. (2012) used ECHAM-HAM which shares the same default $f_{\mathrm{SO_4}}$ assumptions as UKESM from Stier et al. (2005). They investigated the impact on the total shipping radiative forcing of increasing $f_{\mathrm{SO_4}}$ from 2.5 % (Experiment A) to 4.5 % and simultaneously changing primary sulphate to be all in Aitken mode with $D_p = 60\,\mathrm{nm}$ (Experiment B). Using an emission inventory with $8.0\,\mathrm{Tg\,SO_2\,yr^{-1}}$ (which is the same as our modelled reduction from IMO2020) they found this change increased the total radiative forcing from shipping from $-0.10\,\mathrm{W\,m^{-2}}$ to $-0.32\,\mathrm{W\,m^{-2}}$ (with shipping emissions at 60–170 m above sea level for all experiments). The $f_{\mathrm{SO_4}}$ changes between these two Peters et al. (2012) experiments is identical to the changes from our *High* to *Ait_High_4.5* experiments and our IMO2020 ERF increase from $+0.14\,\mathrm{W\,m^{-2}}$ to $+0.31\,\mathrm{W\,m^{-2}}$ between these two experiments agrees well with this result.

Partanen et al. (2013) allocate 100 % of shipping primary sulphate to Aitken mode with $D_p = 88\,\mathrm{nm}$ for all their experiments used to estimate shipping aerosol forcing. Using this $f_{\mathrm{SO_4}}$ size, $f_{\mathrm{SO_4}} = 2.5\,\%$ and emissions in the lowest model layer they find an IMO2020 ERF of $0.33\,\mathrm{W\,m^{-2}}$; this experiment has identical parameters to our *Ait_88nm* experiment which finds an ERF estimate of $0.26 \pm 0.04\,\mathrm{W\,m^{-2}}$, meaning that the difference in primary sulphate size explains a large portion of this discrepancy between the recent IMO2020 estimates in UKESM and Partanen's higher estimate. Another important factor is their use of an emission inventory with a higher percentage (88 %) and absolute ($11.1\,\mathrm{Tg\,yr^{-1}}$) SO_2 reduction compared to ours (77 % and $8.0\,\mathrm{Tg\,yr^{-1}}$) which would be expected to result in a larger forcing. Partanen et al. (2013) also find that increasing $f_{\mathrm{SO_4}}$ from 2.5 % to 4.5 % increases the total radiative effect of shipping emissions from -0.39 to $-0.50\,\mathrm{W\,m^{-2}}$ for their emission inventory with $12.5\,\mathrm{Tg\,SO_2\,yr^{-1}}$.

Both the sign and magnitude of the sensitivity to shipping primary sulphate size and fraction that we have found in UKESM1.1 are well supported by the available prior work, these results are summarised in Table A1. Our results indicate that a significant portion of the difference between the higher IMO2020 forcing values from Partanen et al. (2013) and Lauer et al. (2009) compared to recent model estimates (Fig. 1) can be explained by the smaller assumed shipping emission primary sulphate size in their experiments.

4.3 Why do all recent studies agree on the magnitude of the IMO2020 radiative forcing?

A review of all the published IMO2020 model estimates reveals that all (except Lauer et al. (2009) and Partanen et al. (2013) who found an ERF $> 0.3\,\mathrm{W\,m^{-2}}$) are subject to one or both of the following methodological limitations.

First is the reliance on restrictive emission setups. Most global climate models (GCMs) assume that shipping emissions are injected entirely into the lowest model level, apply a fixed 2.5 % primary sulphate fraction, and emit particles either solely into the accumulation mode or split them with the coarse mode (Table A1). ECHAM (Gettelman et al., 2024) relies on the same default primary sulphate parameterisation as UKESM, originating from Stier et al. (2005) (Zhang et al., 2012; Tegen et al., 2019). Similarly, three estimates from CESM2 (Danabasoglu et al., 2020) assign 100 % of primary sulphate to the accumulation mode with a D_p of 155 nm. This size was explicitly selected by Liu et al. (2012) to match the number of emissions per unit

https://doi.org/10.5194/egusphere-2026-2654
Preprint. Discussion started: 20 May 2026

mass in the Stier et al. (2005) coarse/accumulation split, a decision carried forward into subsequent model versions (Tilmes et al., 2015; Emmons et al., 2020). Consequently, the shipping SO_4 number emission changes resulting from our sensitivity experiments apply directly to ECHAM, CESM, and UKESM variants (using UKCA), which together account for 8 of the 10 GCM ERF estimates published since 2018 (Fig. 1). The two other GCM ERF estimates face similar constraints. NorESM (Skeie et al., 2024) assigns all primary sulphate to the accumulation mode with D_p = 150 nm (Kirkevåg et al., 2018; Seland et al., 2020). Yuan et al. (2024) derived detailed aerosol fields from GEOS-GOCART bulk mass data using a neural network emulator (MAMnet) trained on MAM7. Because MAM7 inherits the same primary sulphate parameters as CESM from Liu et al. (2012), any structural biases regarding aerosol number and size distributions from this are propagated directly into MAMnet and so Yuan et al.'s results. The widespread use of the same shipping emission assumptions, particularly governing emitted aerosol number helps explain why all of the recent seemingly independent model estimates agree so well on the magnitude of the IMO2020 ERF.

The second limitation is the use of model configurations that structurally exclude macrophysical cloud adjustments, and so cannot diagnose the full ERF. The estimates from Bilsback et al. (2020), Sofiev et al. (2018) and OsloCTM3 and NASA GISS ModelE in Skeie et al. (2024) are constrained to capturing only the instantaneous cloud-albedo (Twomey) effect. This conflicts with the Intergovernmental Panel on Climate Change (IPCC) standard for evaluating ERF. The standard framework requires free running GCM simulations with fixed sea surface temperatures (SSTs) precisely to capture the atmosphere's full response (Forster et al., 2016; Bellouin et al., 2020). Rapid adjustments to liquid water path (LWP) and cloud fraction have been repeatedly highlighted as a significant portion of the total aerosol-cloud forcing signal (Chen et al., 2024; Gryspeerdt et al., 2020; Yuan et al., 2023). While GCMs including UKESM1 struggle to represent these adjustments accurately (Malavelle et al., 2017; Mülmenstädt et al., 2024b, a; Grosvenor and Carslaw, 2020) this will be a net positive contribution to the IMO2020 CRE and we have shown it to be particularly important under updated emission parameters (Fig. 4c, f). Therefore excluding it entirely will lead to underestimation of the IMO2020 ERF.

These restrictive emission parameterisations in GCMs and the exclusion of macrophysical contributions has likely led to a systematic underestimation of the IMO2020 ERF in the recent literature.

4.4 Comparison to observations

It is important to reconcile our higher ERF estimates with recent observational studies that have used satellite data to estimate the realised cloud forcing from IMO2020.

Zhang et al. (2025) used an ensemble of 100 neural networks to isolate the IMO2020 signal from satellite measurements over three marine stratocumulus regions. Table 2 compares the regional mean ΔCRE values from their satellite-derived analysis, which accounts for cloud brightness and cloud fraction changes, to our *Base* and *Ait_10* experiments over the same regions. The *Base* experiment underestimates these observational values by over an order of magnitude across all three regions, while *Ait_10* captures the correct order of magnitude but still underestimates by roughly a factor of two. Zhang et al. (2025) also report a global forcing estimate of 0.074 W m^{-2}, but this figure is calculated by assuming zero forcing outside their three analysis regions, which together cover only ~4.2 % of the global surface area. It therefore represents the contribution of these

https://doi.org/10.5194/egusphere-2026-2654
Preprint. Discussion started: 20 May 2026

three regions to the global IMO2020 ERF rather than a global constraint, and is consistent with a substantially larger total forcing once contributions from other areas are included.

Table 2. Regional mean net ΔCRE ($W\,m^{-2}$) comparison between satellite-derived estimates and our *Base* and *Ait_10* UKESM1.1 experiments. Absolute regional forcing values for the Zhang et al. (2025) analysis regions were provided directly by the authors (J. Zhang, personal communication, 2026), as they cannot be precisely derived from the published text alone. All regional means for both the satellite estimates and the model experiments were calculated using exclusively ocean-only grid points within the following bounding boxes: Northeast Pacific (NEP; 10°–40° N, 155°–115° W), Southeast Pacific (SEP; 40°–0° S, 100°–70° W), and Southeast Atlantic (SEA; 25°–0° S, 15° W–15° E).

Region	Zhang et al. (2025)	Base (ERF = 0.10 $W\,m^{-2}$)	Ait_10 (ERF = 0.41 $W\,m^{-2}$)
Northeast Pacific (NEP)	2.29	0.13	0.90
Southeast Pacific (SEP)	0.79	0.18	0.47
Southeast Atlantic (SEA)	2.39	0.06	0.99

Diamond (2023) applied a universal kriging algorithm to MODIS satellite retrievals to estimate the local first indirect effect from IMO2020 over a shipping corridor in the Southeast Atlantic (SEA), finding a forcing of $\sim$2 $W\,m^{-2}$ in September–October–November (SON) and $\sim$0.5 $W\,m^{-2}$ in the annual mean over the corridor. These estimates capture the first indirect effect only and assume clean reference conditions outside the corridor, so represent a lower bound on the total regional shipping ΔCRE.

In our *Base* experiment the corridor-mean ΔCRE is 0.34 $W\,m^{-2}$ in SON and 0.13 $W\,m^{-2}$ in the annual mean, well below Diamond's estimates. In *Ait_10* it rises to 2.4 $W\,m^{-2}$ (SON) and 1.3 $W\,m^{-2}$ (annual), comparable in magnitude to Diamond's SON value although potentially overestimating the annual mean. Direct comparison is complicated by SO_2 inventory differences (Fig. S6) and by the coarse resolution of N96 ($\sim$135 km) output over a region only a few grid cells wide.

Possner et al. (2016) showed that GCM-scale emission dilution can overestimate ship-induced SW CRE through loss of sub-grid N_d variability, suggesting experiments matching Diamond's corridor ΔCRE may overestimate the gobal forcing. However, the comparison with Zhang et al. (2025) indicates that any resolution-driven overestimate in our simulations is not large enough to undermine the case for an upward revision.

Gettelman et al. (2024) demonstrated a "significant but weak" spatial correlation of 0.26 between the CERES CRE anomaly and the CESM2 IMO2020 ΔCRE over the Northern Hemisphere (20–70°N, ocean only), exceeding the one standard deviation range of pre-2020 random correlations. Here we replicate their methodology; Figure 5 shows the results. We find NH correlations of 0.29, 0.14, and 0.37 for CESM2, *Base*, and *Ait_10* respectively, all exceeding the one standard deviation threshold. The higher CESM2 correlation relative to *Base* likely reflects better isolation of the IMO2020 signal in nudged simulations. Over the SEA, *Base* and CESM2 correlations are indistinguishable from variability, whereas *Ait_10* is 0.47, exceeding the range of expected random values (Fig.5d). This means that under default emission parameters, IMO2020 cannot explain the observed regional CRE anomaly over the SEA, but with updated primary SO_4 in UKESM1.1 a clear spatial fingerprint emerges.

https://doi.org/10.5194/egusphere-2026-2654
Preprint. Discussion started: 20 May 2026

Hansen et al. (2025) argued based on observations that the IMO2020 ERF was of the order of 0.5 W m^{-2}. While this estimate has been scrutinised for potentially conflating aerosol forcing with coupled SST–cloud feedbacks, our results identify a mechanism which can reconcile the difference between this top-down inference and lower estimates from recent model experiments.

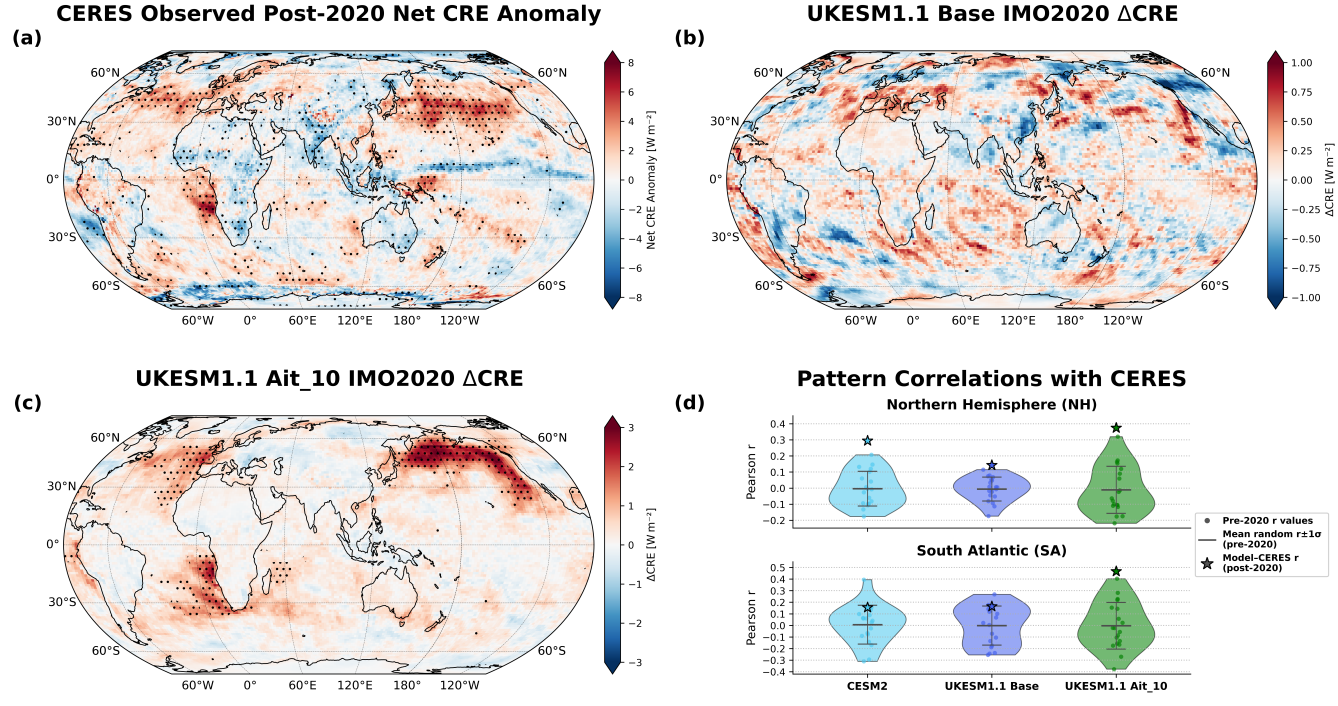

Figure 5. Annual mean observed CERES net CRE anomaly (2020–2025 relative to 2002–2019 climatology) (a) and net IMO - CTL ΔCRE from *Base* (b) and *Ait_10* (c). (d) Pattern correlations between each experiment's net ΔCRE from IMO2020 (including CESM2 from Gettelman (2024)) and post-2020 CERES anomalies. Violins show the null distribution from correlations against individual pre-2020 CERES years. Note the different map colour scales. Stippling denotes regions significant at the 90 % (model) and 95 % (CERES) confidence levels, using the Benjamini–Hochberg False Discovery Rate (FDR) correction (Wilks, 2006, 2016).

In summary, our experiments with updated emission parameters bring the modelled regional ΔCRE closer to satellite-derived estimates with some evidence suggesting that even our *Ait_10* experiment with an ERF of 0.41 W m^{-2} is underestimating the ΔCRE from IMO2020. Recent modelling studies report 0.04–0.14 °C of additional global warming by 2030 attributed to IMO2020 (Jordan and Henry, 2024; Quaglia and Visioni, 2024; Gettelman et al., 2024; Watson-Parris et al., 2025; Yoshioka et al., 2024), based on ERFs of 0.12–0.14 W m^{-2} (Figure 1). Our higher ERF range would imply a substantially larger warming impact attributable to IMO2020, although coupled simulations, ideally from multiple models, would be required to quantify this fully.

https://doi.org/10.5194/egusphere-2026-2654
Preprint. Discussion started: 20 May 2026

5 Conclusions

We have demonstrated that the IMO2020 effective radiative forcing is highly sensitive to model assumptions controlling the number, size, and vertical distribution of sulphate aerosol emitted from shipping. In UKESM1.1 reallocating shipping primary sulphate from accumulation and coarse modes to Aitken mode, consistent with ship exhaust observations, increases the IMO2020 ERF from $0.10\,\mathrm{W\,m^{-2}}$ to between 0.19 and $0.31\,\mathrm{W\,m^{-2}}$, driven by an order-of-magnitude (10–79x) increase in modelled aerosol number emissions for the same sulphur mass. Additionally increasing the primary sulphate fraction from 2.5 to 10 % yields an ERF of $0.41\,\mathrm{W\,m^{-2}}$ from further increasing aerosol number emissions. We also find a consistent but uncertain positive ERF increase from increasing emission altitude which combines with increases from primary sulphate changes.

These results are well supported by previous studies using climate models with independent lineage to UKESM1.1. Our results indicate that differences in assumed primary sulphate size explains the majority of the discrepancy between earlier higher estimates of the IMO2020 forcing and the recent consensus near $0.1\,\mathrm{W\,m^{-2}}$. However the magnitude of the sensitivities identified here will likely vary between models due to differences in updraft velocities (Virtanen et al., 2025), and the community would benefit from further investigation with other CMIP6 and later generation climate models.

Our higher ERF estimates are also supported by comparison to observations: updated emission parameters bring the modelled regional ΔCRE substantially closer to published satellite-derived estimates and improve spatial correlations with observed CERES anomalies. Some discrepancy with these satellite-derived estimates remains, although close agreement is not necessarily expected given the inherent methodological differences between coarse-resolution global model output and satellite-derived regional estimates. Continued observational constraints on IMO2020 are an important avenue for future work.

All recent GCM estimates of the IMO2020 ERF use accumulation or coarse mode primary sulphate, low primary sulphate fraction (2.5%), and lowest-level emission injection, all of which we have shown to suppress the modelled IMO2020 ERF. The fundamental reason this bias will carry across models is physical: any model that represents the Twomey effect will produce a larger cloud forcing in response to a large increase in CCN-active aerosol number. We therefore conclude that, due to these shared assumptions, recent climate model estimates of the Effective Radiative Forcing and thus the resulting warming from the IMO2020 shipping regulations has been systematically underestimated and is larger and less well constrained than the convergence to $\sim$0.1 $\mathrm{W\,m^{-2}}$ in the literature suggests. However we emphasise that all GCMs, including ours, are subject to common resolution-imposed limitations on the representation of aerosol–cloud interactions.

Our results suggest that the forcing is 2 to 4 times larger than the current consensus, if true this would correspond to a significantly larger warming impact from IMO2020 than is currently recognised. Based on the potential importance of this result, it is recommended that other models perform experiments using an identical framework to assess the multi-model response to IMO shipping regulation changes under improved emission assumptions.

https://doi.org/10.5194/egusphere-2026-2654
Preprint. Discussion started: 20 May 2026

Appendix A: Summary of emission assumptions in prior IMO2020 modelling studies

Table A1: Results and assumptions from previous IMO2020 modelling studies.

Reference	ERF/RF ($W\,m^{-2}$)	Model	Activation scheme	ΔSO_2 ($Tg\,yr^{-1}$)	ΔSO_2 (%)	Height	f_{SO_4} (%)	Primary SO_4 size (modal split, D_p)
Base_ARG2000	0.097	UKESM1.1	ARG	8.0	77.3	∼20 m	2.5	50% Acc. (150nm), 50% Coarse (1500nm)
Base	0.100	UKESM1.1	ARG-G25	8.0	77.3	∼20 m	2.5	50% Acc. (150nm), 50% Coarse (1500nm)
High	0.136	UKESM1.1	ARG-G25	8.0	77.3	100–320 m	2.5	50% Acc. (150nm), 50% Coarse (1500nm)
High_4.5	0.164	UKESM1.1	ARG-G25	8.0	77.3	100–320 m	4.5	50% Acc. (150nm), 50% Coarse (1500nm)
Ait	0.187	UKESM1.1	ARG-G25	8.0	77.3	20 m	2.5	100% Aitken (60 nm)
Ait_88nm	0.256	UKESM1.1	ARG-G25	8.0	77.3	∼20 m	2.5	100% Aitken (88 nm)
Ait_44nm	0.309	UKESM1.1	ARG-G25	8.0	77.3	∼20 m	2.5	100% Aitken (44 nm)
Ait_High	0.270	UKESM1.1	ARG-G25	8.0	77.3	100–320 m	2.5	100% Aitken (60 nm)
Ait_High_4.5	0.309	UKESM1.1	ARG-G25	8.0	77.3	100–320 m	4.5	100% Aitken (60 nm)
Ait_10	0.407	UKESM1.1	ARG-G25	8.0	77.3	∼20 m	10	100% Aitken (60 nm)
Jordan and Henry (2024)	0.139	UKESM1	ARG	9.9	85.7	∼20 m	2.5	50% Acc. (150nm), 50% Coarse (1500nm)
Yoshioka et al. (2024)	0.128	HadGEM-GC3.1	ARG	8.0	80	∼20 m	2.5	50% Acc. (150nm), 50% Coarse (1500nm)
Gettelman et al. (2024)	0.11	CESM2	ARG	8.0	80	ML1 ∼40 m	2.5	100% Acc. (155 nm)
Gettelman et al. (2024)	0.14	UKCA (UKESM1)	ARG	8.0	80	∼20 m	2.5	50% Acc. (150nm), 50% Coarse (1500nm)
Gettelman et al. (2024)	0.15	ECHAM	ARG	8.0	80	ML1	2.5	50% Acc. (150nm), 50% Coarse (1500nm)
Quaglia and Visioni (2024)	0.14	CESM2	ARG	8.4	90	ML1 ∼40 m	2.5	100% Acc. (155 nm)
Skeie et al. (2024)	0.085	CESM2	ARG	8.7	80	ML1 ∼40 m	2.5	100% Acc. (155 nm)
Skeie et al. (2024)	0.065	GISS ModelE_MATRIX	ARG	8.7	80	ML1	2.5	99% Acc. (68 nm), 1% Ait. (13 nm)
Skeie et al. (2024)	0.08	GISS ModelE_OMA	NA	8.7	80	ML1	2.5	NA
Skeie et al. (2024)	0.065	NorESM2	ARG	8.7	80	ML1	2.5	100% Acc. (150 nm)
Skeie et al. (2024)	0.07	OsloCTM3	NA	8.7	80	ML1	2.5	NA
Yuan et al. (2024)	0.14	GEOS-GOCART	ARG	7.4	85	ML1	2.5	NA
Bilsback et al. (2020)	0.027	GEOS-Chem-TOMAS	NA	7.6	85	ML1	3.1	Bimodal (10 nm and 70 nm)
Jin et al. (2018)	0.226	CESM1.2.2	ARG	12.0	85.7	ML1 ∼40 m	2.5	100% Acc. (155 nm)
Jin et al. (2018)	0.185	CESM1.2.2	ARG	8.8	81.4	ML1 ∼40 m	2.5	100% Acc. (155 nm)
Sofiev et al. (2018)	0.071	FMI SILAM5.5	NA	8.5	77	ML1	0.4 to 3	NA
Partanen et al. (2013)	0.33	ECHAM-HAMMOZ	ARG	11.1	88.6	ML1	2.5	100% Aitken (88 nm)
Partanen et al. (2013)	0.39	ECHAM-HAMMOZ	ARG	12.5	100	ML1	2.5	100% Aitken (88 nm)
Partanen et al. (2013)	0.50	ECHAM-HAMMOZ	ARG	12.5	100	ML1	4.5	100% Aitken (88 nm)
Partanen et al. (2013)	0.43	ECHAM-HAMMOZ	ARG	13.1	100	ML1	2.5	100% Aitken (88 nm)
Partanen et al. (2013)	0.54	ECHAM-HAMMOZ	ARG	13.1	100	ML1	4.5	100% Aitken (88 nm)
Partanen et al. (2013)	0.53	ECHAM-HAMMOZ	ARG	17.4	100	ML1	2.5	100% Aitken (88 nm)

https://doi.org/10.5194/egusphere-2026-2654
Preprint. Discussion started: 20 May 2026

Reference	ERF/RF ($W\,m^{-2}$)	Model	Act. scheme	SO_2 red. ($Tg\,yr^{-1}$)	Red. (%)	Height	f_{SO_4} (%)	Primary SO_4 size (modal split, D_p)
Peters et al. (2012) A	0.102	ECHAM5-HAM2	LL1997	8.0	100	60–170 m	2.5	50% Acc. (150nm), 50% Coarse (1500nm)
Peters et al. (2012) B	0.321	ECHAM5-HAM2	LL1997	8.0	100	60–170 m	4.5	100% Aitken (60 nm)
Peters et al. (2012) Asc	0.148	ECHAM5-HAM2	LL1997	13.0	100	60–170 m	2.5	50% Acc. (150nm), 50% Coarse (1500nm)
Peters et al. (2012) Bsc	0.486	ECHAM5-HAM2	LL1997	13.0	100	60–170 m	4.5	100% Aitken (60 nm)
Righi et al. (2011)	0.28	EMAC-MADE	ARG	14.0	100	ML1	2.5	80% Ait. (70 nm), 20% Acc. (260 nm)
Righi et al. (2011)	0.32	EMAC-MADE	ARG	14.0	100	ML1	2.5	96% Ait. (58 nm), 4% Acc. (310 nm)
Righi et al. (2011)	0.40	EMAC-MADE	ARG	14.0	100	ML1	2.5	100% Aitken (30 nm)
Lauer et al. (2007) EXPA	0.61	ECHAM5/MESSy1	ARG	11.7	100	ML1	4.4	100% Aitken (30 nm)
Lauer et al. (2007) EXPC	0.46	ECHAM5/MESSy1	ARG	9.4	100	ML1	2.5	100% Aitken (30 nm)
Lauer et al. (2007) EXPB	0.20	ECHAM5/MESSy1	ARG	7.8	100	ML1	2.5	100% Aitken (30 nm)
Lauer et al. (2009)	0.59	ECHAM5/MESSy1	ARG	13.75	100	ML1	2.5	100% Aitken (30 nm)
Lauer et al. (2009)	0.307	ECHAM5/MESSy1	ARG	11.2	81.5	ML1	2.5	100% Aitken (30 nm)
Capaldo et al. (1999)	0.11	GFDL CTM	NA	8.4	100	ML1	2.5	NA

Notes for Table A1:

1. Where emission assumption information was not provided in the original study, model configurations were assumed to be those from the relevant model documentation or corresponding authors were contacted.

2. The model documentation used for UKCA is listed in section 3.1 and references used for many of the other studies can be found in 4.3. Additional references used not listed above are: Bauer et al. (2020), Kelley et al. (2020), Bauer et al. (2008), Lee et al. (2015).

3. ML1 refers to the lowest model level. "NA" in the primary SO_4 size column indicates that the model uses a bulk representation of sulphate aerosol and size parameters do not exist.

4. Many older estimates are total shipping emission radiative forcing, reported as negative in the original papers. Here all values have been converted to the equivalent ERF for a reduction in shipping emissions so that the sign convention matches IMO2020 ERF estimates.

5. NASA GISS ModelE_OMA uses an empirical N_d calculation following Menon and Rotstayn (2006). Both ModelE_OMA and OsloCTM3 (Skeie et al., 2024) use bulk tracers for SO_2 and SO_4, so sulphate size does not vary interactively. GEOS-GOCART (Yuan et al., 2024) also uses a bulk sulphate representation with a single tracer, see main text 4.3 for details.

6. Peters et al. (2012) use the Lin and Leaitch (1997) activation scheme in their configuration of ECHAM5-HAM2. This reference refers to conference proceedings (WMO Workshop on Measurement of Cloud Properties for Forecasts of

https://doi.org/10.5194/egusphere-2026-2654
Preprint. Discussion started: 20 May 2026

Weather, Air Quality and Climate, Mexico City, 328–335) and does not appear to be publicly available. Later versions of ECHAM use the ARG scheme.

7. Righi et al. (2011) additionally varied geometric standard deviations of accumulation and Aitken mode primary sulphate emissions between experiments based on Petzold et al. (2008), whereas other studies including ours kept these fixed.

8. Bilsback et al. (2020) do not state how f_{SO_4} mass is split between their two modes.

9. Sofiev et al. (2018) use the STEAM emission inventory in FMI SILAM5.5 which uses a variable primary sulphate fraction between 0.4 and 3%.

Code and data availability

The processed model output data from our experiments and analysis scripts are available at Smith (2026). CESM2 IMO2020 experiment data used is available at Gettelman (2024). Observational Top of Atmosphere Cloud Radiative Effect (CRE) data used in this study were obtained from the Clouds and the Earth's Radiant Energy System (CERES) Energy Balanced and Filled (EBAF) Top-of-Atmosphere (TOA) Edition 4.2 dataset (Loeb et al., 2018).

Author contributions

JH and MH conceived the initial study premise, JS expanded the research scope, developed the central scientific narrative, and incorporated key ideas from MY. JS set up and ran the UKESM1.1 simulations with contributions from BJ and MH. JS conducted the data analysis and wrote the manuscript. All authors reviewed and provided comments on the manuscript.

Competing interests

None of the authors have any competing interests.

Acknowledgements

We would like to thank Andy Jones for his work incorporating the updated ARG-G25 activation scheme into the UKESM1.1 configurations used here and for his expertise on UKCA and the UM. We thank Charlie Wartnaby for his work making the CMIP7 emission datasets used here available early. We thank Jianhao Zhang for his helpful replies and for sharing statistics from his work. We also thank Axel Lauer, Qinjian Jin and James Corbett for their prompt and helpful responses to questions regarding the emission setups used in their prior work on shipping. We acknowledge the use of generative AI for assistance with python coding syntax. Model simulations were performed using the Met Offices supercomputing facilities.

Financial support

Support for JS and JH was provided by Quadrature Climate Foundation (QCF). MH was supported by Silver Lining's Safe Climate Research Initiative (SCRI). BJ was supported by the Hadley Centre Climate Programme funded by the Department for Science Imovation and Technology. For the purpose of open access, the author has applied a Creative Commons Attribution (CC BY) licence to any Author Accepted Manuscript version arising.

https://doi.org/10.5194/egusphere-2026-2654
Preprint. Discussion started: 20 May 2026

References

Abdul-Razzak, H. and Ghan, S. J.: A parameterization of aerosol activation: 2. Multiple aerosol types, Journal of Geophysical Research: Atmospheres, 105, 6837–6844, https://doi.org/10.1029/1999JD901161, 2000.

Ackerman, A. S., Kirkpatrick, M. P., Stevens, D. E., and Toon, O. B.: The impact of humidity above stratiform clouds on indirect aerosol climate forcing, Nature, 432, 1014–1017, https://doi.org/10.1038/nature03137, 2004.

Agrawal, H., Welch, W. A., Miller, J. W., and Cocker, D. R.: Emission Measurements from a Crude Oil Tanker at Sea, Environmental Science & Technology, 42, 7098–7103, https://doi.org/10.1021/es703102y, 2008.

Agrawal, H., Welch, W. A., Henningsen, S., Miller, J. W., and Cocker, D. R.: Emissions from main propulsion engine on container ship at sea, Journal of Geophysical Research: Atmospheres, 115, 2009JD013 346, https://doi.org/10.1029/2009JD013346, 2010.

Ahsan, H., Wang, H., Wu, J., Wu, M., Smith, S. J., Bauer, S., Suchyta, H., Olivié, D., Myhre, G., Matsui, H., Bian, H., Lamarque, J.-F., Carslaw, K., Horowitz, L., Regayre, L., Chin, M., Schulz, M., Skeie, R. B., Takemura, T., and Naik, V.: The Emissions Model Intercomparison Project (Emissions-MIP): quantifying model sensitivity to emission characteristics, Atmospheric Chemistry and Physics, 23, 14 779–14 799, https://doi.org/10.5194/acp-23-14779-2023, 2023.

Albrecht, B. A.: Aerosols, cloud microphysics, and fractional cloudiness, Science, 245, 1227–1230, https://doi.org/10.1126/science.245.4923.1227, 1989.

Archibald, A. T., O'Connor, F. M., Abraham, N. L., et al.: Description and evaluation of the UKCA stratosphere–troposphere chemistry scheme (StratTrop) – Part 1: Physics and atmospheric dynamics, Geoscientific Model Development, 13, 1223–1266, https://doi.org/10.5194/gmd-13-1223-2020, 2020.

Badeke, R., Matthias, V., Karl, M., and Grawe, D.: Effects of vertical ship exhaust plume distributions on urban pollutant concentration – a sensitivity study with MITRAS v2.0 and EPISODE-CityChem v1.4, Geoscientific Model Development, 15, 4077–4103, https://doi.org/10.5194/gmd-15-4077-2022, 2022.

Bauer, S. E., Wright, D. L., Koch, D., Lewis, E. R., McGraw, R., Chang, L.-S., Schwartz, S. E., and Ruedy, R.: MATRIX (Multiconfiguration Aerosol TRacker of mIXing state): an aerosol microphysical module for global atmospheric models, Atmospheric Chemistry and Physics, 8, 6003–6035, https://doi.org/10.5194/acp-8-6003-2008, 2008.

Bauer, S. E., Tsigaridis, K., Faluvegi, G., Kelley, M., Lo, K. K., Miller, R. L., Nazarenko, L., Schmidt, G. A., and Wu, J.: Historical (1850–2014) Aerosol Evolution and Role on Climate Forcing Using the GISS ModelE2.1 Contribution to CMIP6, Journal of Advances in Modeling Earth Systems, 12, e2019MS001 978, https://doi.org/10.1029/2019MS001978, 2020.

Bellouin, N., Quaas, J., Gryspeerdt, E., Kinne, S., Stier, P., Watson-Parris, D., Boucher, O., Carslaw, K. S., Christensen, M., Danez, A.-L., et al.: Bounding global aerosol radiative forcing of climate change, Reviews of Geophysics, 58, e2019RG000 660, https://doi.org/10.1029/2019RG000660, 2020.

Bilsback, K. R., Kerry, D., Croft, B., Ford, B., Jathar, S. H., Carter, E., Martin, R. V., and Pierce, J. R.: Beyond SO_x reductions from shipping: assessing the impact of NO_x and carbonaceous-particle controls on human health and climate, Environmental Research Letters, 15, 124 046, https://doi.org/10.1088/1748-9326/abc718, 2020.

Borén, C., Fridell, E., and Ingelsten, H.: Ship emission measurements and analysis, Transportation Research Part D: Transport and Environment, 118, 103 722, https://doi.org/10.1016/j.trd.2023.103722, 2023.

Bretherton, C. S., Blossey, P. N., and Uchida, J.: Cloud droplet sedimentation, entrainment efficiency, and subtropical stratocumulus albedo, Geophysical Research Letters, 34, https://doi.org/10.1029/2006GL027648, 2007.

https://doi.org/10.5194/egusphere-2026-2654
Preprint. Discussion started: 20 May 2026

Briggs, G. A.: A Plume Rise Model Compared with Observations, Journal of the Air Pollution Control Association, 15, 433–438, https://doi.org/10.1080/00022470.1965.10468404, 1965.

Capaldo, K., Corbett, J. J., Kasibhatla, P., Fischbeck, P., and Pandis, S. N.: Effects of ship emissions on sulphur cycling and radiative climate forcing over the ocean, Nature, 400, 743–746, https://doi.org/10.1038/23438, 1999.

Chen, Y., Haywood, J., Wang, Y., Malavelle, F., Jordan, G., Partridge, D., Fieldsend, J., De Leeuw, J., Schmidt, A., Cho, N., Oreopoulos, L., Platnick, S., Grosvenor, D., Field, P., and Lohmann, U.: Machine learning reveals climate forcing from aerosols is dominated by increased cloud cover, Nature Geoscience, 15, 609–614, https://doi.org/10.1038/s41561-022-00991-6, 2022.

Chen, Y., Haywood, J., Wang, Y., Malavelle, F., Jordan, G., Peace, A., Partridge, D. G., Cho, N., Oreopoulos, L., Grosvenor, D., Field, P., Allan, R. P., and Lohmann, U.: Substantial cooling effect from aerosol-induced increase in tropical marine cloud cover, Nature Geoscience, 17, 404–410, https://doi.org/10.1038/s41561-024-01427-z, 2024.

Chosson, F., Paoli, R., and Cuenot, B.: Ship plume dispersion rates in convective boundary layers for chemistry models, Atmospheric Chemistry and Physics, 8, 4841–4853, https://doi.org/10.5194/acp-8-4841-2008, 2008.

Corbett, J. J., Winebrake, J. J., Carr, E. W., Jalkanen, J.-P., Johansson, L., Prank, M., and Sofiev, M.: Health Impacts Associated with Delay of MARPOL Global Sulphur Standards, https://wwwcdn.imo.org/localresources/en/MediaCentre/HotTopics/Documents/Finland%20study%20on%20health%20benefits.pdf, last access: 29 March 2026, 2016.

Corbin, J. C., Mensah, A. A., Pieber, S. M., Orasche, J., Michalke, B., Zanatta, M., Czech, H., Massabò, D., Buatier De Mongeot, F., Mennucci, C., El Haddad, I., Kumar, N. K., Stengel, B., Huang, Y., Zimmermann, R., Prévôt, A. S. H., and Gysel, M.: Trace Metals in Soot and $PM_{2.5}$ from Heavy-Fuel-Oil Combustion in a Marine Engine, Environmental Science & Technology, 52, 6714–6722, https://doi.org/10.1021/acs.est.8b01764, 2018.

Danabasoglu, G., Lamarque, J.-F., Bacmeister, J., Bailey, D. A., DuVivier, A. K., Edwards, J., Emmons, L. K., Fasullo, J., Garcia, R., Gettelman, A., Hannay, C., Holland, M. M., Large, W. G., Lauritzen, P. H., Lawrence, D. M., Lenaerts, J. T. M., Lindsay, K., Lipscomb, W. H., Mills, M. J., Neale, R., Oleson, K. W., Otto-Bliesner, B., Phillips, A. S., Sacks, W., Tilmes, S., Van Kampenhout, L., Vertenstein, M., Bertini, A., Dennis, J., Deser, C., Fischer, C., Fox-Kemper, B., Kay, J. E., Kinnison, D., Kushner, P. J., Larson, V. E., Long, M. C., Mickelson, S., Moore, J. K., Nienhouse, E., Polvani, L., Rasch, P. J., and Strand, W. G.: The Community Earth System Model Version 2 (CESM2), Journal of Advances in Modeling Earth Systems, 12, e2019MS001 916, https://doi.org/10.1029/2019MS001916, 2020.

Dentener, F., Kinne, S., Bond, T., Boucher, O., Cofala, J., Generoso, S., Ginoux, P., Gong, S., Hoelzemann, J. J., Ito, A., Marelli, L., Penner, J. E., Putaud, J.-P., Textor, C., Schulz, M., van der Werf, G. R., and Wilson, J.: Emissions of primary aerosol and precursor gases in the years 2000 and 1750 prescribed data-sets for AeroCom, Atmospheric Chemistry and Physics, 6, 4321–4344, https://doi.org/10.5194/acp-6-4321-2006, 2006.

Diamond, M. S.: Detection of large-scale cloud microphysical changes within a major shipping corridor after implementation of the International Maritime Organization 2020 fuel sulfur regulations, Atmospheric Chemistry and Physics, 23, 8259–8269, https://doi.org/10.5194/acp-23-8259-2023, 2023.

Ding, X., Li, Q., Wu, D., Wang, X., Li, M., Wang, T., Wang, L., and Chen, J.: Direct Observation of Sulfate Explosive Growth in Wet Plumes Emitted From Typical Coal-Fired Stationary Sources, Geophysical Research Letters, 48, e2020GL092 071, https://doi.org/10.1029/2020GL092071, 2021.

Emmons, L. K., Schwantes, R. H., Orlando, J. J., Tyndall, G., Kinnison, D., Lamarque, J.-F., Marsh, D., Mills, M. J., Tilmes, S., Bardeen, C., Buchholz, R. R., Conley, A., Gettelman, A., Garcia, R., Simpson, I., Blake, D. R., Meinardi, S., and Pétron, G.: The Chemistry Mechanism

https://doi.org/10.5194/egusphere-2026-2654
Preprint. Discussion started: 20 May 2026

in the Community Earth System Model Version 2 (CESM2), Journal of Advances in Modeling Earth Systems, 12, e2019MS001 882, https://doi.org/10.1029/2019MS001882, 2020.

Forster, P. M., Richardson, T., Maycock, A. C., Smith, C. J., Samset, B. H., Myhre, G., Andrews, T., Pincus, R., and Schulz, M.: Recommendations for diagnosing effective radiative forcing from climate models for CMIP6, Journal of Geophysical Research: Atmospheres, 121, https://doi.org/10.1002/2016JD025320, 2016.

Gan, L., Lu, T., and Shu, Y.: Diffusion and Superposition of Ship Exhaust Gas in Port Area Based on Gaussian Puff Model: A Case Study on Shenzhen Port, Journal of Marine Science and Engineering, 11, 330, https://doi.org/10.3390/jmse11020330, 2023.

Gettelman, A.: Simulations and Analysis In Support of "Has Reducing Ship Emissions Brought Forward Global Warming?", https://doi.org/10.5281/zenodo.10724917, 2024.

Gettelman, A., Christensen, M. W., Diamond, M. S., Gryspeerdt, E., Manshausen, P., Stier, P., Watson-Parris, D., Yang, M., Yoshioka, M., and Yuan, T.: Has Reducing Ship Emissions Brought Forward Global Warming?, Geophysical Research Letters, 51, https://doi.org/10.1029/2024GL109077, 2024.

Ghan, S. J.: Technical note: Estimating aerosol effects on cloud radiative forcing, Atmospheric Chemistry and Physics, 13, 9971–9974, https://doi.org/10.5194/acp-13-9971-2013, 2013.

Ghan, S. J., Abdul-Razzak, H., Nenes, A., Ming, Y., Liu, X., Ovchinnikov, M., Shipway, B., Meskhidze, N., Xu, J., and Shi, X.: Droplet nucleation: Physically-based parameterizations and comparative evaluation, Journal of Advances in Modeling Earth Systems, 3, https://doi.org/10.1029/2011MS000074, 2011.

Ghosh, P., Evans, K. J., Grosvenor, D. P., Kang, H.-G., Mahajan, S., Xu, M., Zhang, W., and Gordon, H.: Assessing modifications to the Abdul-Razzak and Ghan aerosol activation parameterization (version ARG2000) to improve simulated aerosol–cloud radiative effects in the UK Met Office Unified Model (UM version 13.0), Geoscientific Model Development, 18, 4899–4913, https://doi.org/10.5194/gmd-18-4899-2025, 2025.

Grosvenor, D. P. and Carslaw, K. S.: The decomposition of cloud–aerosol forcing in the UK Earth System Model (UKESM1), Atmospheric Chemistry and Physics, 20, 15 681–15 724, https://doi.org/10.5194/acp-20-15681-2020, 2020.

Gryspeerdt, E., Mülmenstädt, J., Gettelman, A., Malavelle, F. F., Morrison, H., Neubauer, D., Partridge, D. G., Stier, P., Takemura, T., Wang, H., Wang, M., and Zhang, K.: Surprising similarities in model and observational aerosol radiative forcing estimates, Atmospheric Chemistry and Physics, 20, 613–623, https://doi.org/10.5194/acp-20-613-2020, 2020.

Hansen, J. E., Kharecha, P., Sato, M., Tselioudis, G., Kelly, J., Bauer, S. E., Ruedy, R., Jeong, E., Jin, Q., Rignot, E., Velicogna, I., Schoeberl, M. R., Von Schuckmann, K., Amponsem, J., Cao, J., Keskinen, A., Li, J., and Pokela, A.: Global Warming Has Accelerated: Are the United Nations and the Public Well-Informed?, Environment: Science and Policy for Sustainable Development, 67, 6–44, https://doi.org/10.1080/00139157.2025.2434494, 2025.

Hoesly, R. M., Smith, S. J., Feng, L., Klimont, Z., Janssens-Maenhout, G., Pitkanen, T., Seibert, J. J., Vu, L., Andres, R. J., Bolt, R. M., Bond, T. C., Dawidowski, L., Kholod, N., Kurokawa, J.-i., Li, M., Liu, L., Lu, Z., Moura, M. C. P., O'Rourke, P. R., and Zhang, Q.: Historical (1750–2014) anthropogenic emissions of reactive gases and aerosols from the Community Emissions Data System (CEDS), Geoscientific Model Development, 11, 369–408, https://doi.org/10.5194/gmd-11-369-2018, 2018.

IMO: IMO2020: Consistent implementation of MARPOL Annex VI, 2019.

Jalkanen, J.-P., Johansson, L., Kukkonen, J., Brink, A., Kalli, J., and Stipa, T.: Extension of an assessment model of ship traffic exhaust emissions for particulate matter and carbon monoxide, Atmospheric Chemistry and Physics, 12, 2641–2659, https://doi.org/10.5194/acp-12-2641-2012, 2012.

https://doi.org/10.5194/egusphere-2026-2654
Preprint. Discussion started: 20 May 2026

Jin, Q., Grandey, B. S., Rothenberg, D., Avramov, A., and Wang, C.: Impacts on cloud radiative effects induced by coexisting aerosols converted from international shipping and maritime DMS emissions, Atmospheric Chemistry and Physics, 18, 16 793–16 808, https://doi.org/10.5194/acp-18-16793-2018, 2018.

Jonsson, Å. M., Westerlund, J., and Hallquist, M.: Size-resolved particle emission factors for individual ships, Geophysical Research Letters, 38, https://doi.org/10.1029/2011GL047672, 2011.

Jordan, G. and Henry, M.: IMO2020 Regulations Accelerate Global Warming by up to 3 Years in UKESM1, Earth's Future, 12, https://doi.org/10.1029/2024EF005011, 2024.

Kelley, M., Schmidt, G. A., Nazarenko, L. S., Bauer, S. E., Ruedy, R., Russell, G. L., Ackerman, A. S., Aleinov, I., Bauer, M., Bleck, R., Canuto, V., Cesana, G., Cheng, Y., Clune, T. L., Cook, B. I., Cruz, C. A., Del Genio, A. D., Elsaesser, G. S., Faluvegi, G., Kiang, N. Y., Kim, D., Lacis, A. A., Leboissetier, A., LeGrande, A. N., Lo, K. K., Marshall, J., Matthews, E. E., McDermid, S., Mezuman, K., Miller, R. L., Murray, L. T., Oinas, V., Orbe, C., García-Pando, C. P., Perlwitz, J. P., Puma, M. J., Rind, D., Romanou, A., Shindell, D. T., Sun, S., Tausnev, N., Tsigaridis, K., Tselioudis, G., Weng, E., Wu, J., and Yao, M.-S.: GISS-E2.1: Configurations and Climatology, Journal of Advances in Modeling Earth Systems, 12, e2019MS002 025, https://doi.org/10.1029/2019MS002025, 2020.

Kerminen, V.-M., Chen, X., Vakkari, V., Petäjä, T., Kulmala, M., and Bianchi, F.: Atmospheric new particle formation and growth: review of field observations, Environmental Research Letters, 13, 103 003, https://doi.org/10.1088/1748-9326/aadf3c, 2018.

Khairoutdinov, M. and Kogan, Y.: A new cloud physics parameterization in a large-eddy simulation model of marine stratocumulus, Monthly Weather Review, 128, 229–243, https://doi.org/10.1175/1520-0493(2000)128<0229:ANCPPI>2.0.CO;2, 2000.

Kirkevåg, A., Grini, A., Olivié, D., Seland, Ø., Alterskjær, K., Hummel, M., Karset, I. H. H., Lewinschal, A., Liu, X., Makkonen, R., Bethke, I., Griesfeller, J., Schulz, M., and Iversen, T.: A production-tagged aerosol module for Earth system models, OsloAero5.3 – extensions and updates for CAM5.3-Oslo, Geoscientific Model Development, 11, 3945–3982, https://doi.org/10.5194/gmd-11-3945-2018, 2018.

Klimont, Z., Kupiainen, K., Heyes, C., Purohit, P., Cofala, J., Rafaj, P., Borken-Kleefeld, J., and Schöpp, W.: Global anthropogenic emissions of particulate matter including black carbon, Atmospheric Chemistry and Physics, 17, 8681–8723, https://doi.org/10.5194/acp-17-8681-2017, 2017.

Kuhlbrodt, T., Jones, C. G., Sellar, A., Sherwood, S. C., et al.: The low-resolution version of HadGEM3 GC3.1: development and evaluation for global climate, Journal of Advances in Modeling Earth Systems, 10, 2865–2888, https://doi.org/10.1029/2018MS001370, 2018.

Lauer, A., Eyring, V., Hendricks, J., Jöckel, P., and Lohmann, U.: Global model simulations of the impact of ocean-going ships on aerosols, clouds, and the radiation budget, Atmospheric Chemistry and Physics, 7, 5061–5079, https://doi.org/10.5194/acp-7-5061-2007, 2007.

Lauer, A., Eyring, V., Corbett, J. J., Wang, C., and Winebrake, J. J.: Assessment of Near-Future Policy Instruments for Oceangoing Shipping: Impact on Atmospheric Aerosol Burdens and the Earth's Radiation Budget, Environmental Science & Technology, 43, 5592–5598, https://doi.org/10.1021/es900922h, 2009.

Lee, J. D., Pasternak, D., Wilde, S. E., Drysdale, W. S., Lacy, S. E., Moller, S. J., Shaw, M., Squires, F. A., Edwards, P., Temple, L. G., Coe, H., Wu, H., Batten, S. E., Bauguitte, S., Reed, C., Bell, T. G., Yang, M., Jalkanen, J.-P., and Buhigas, J.: SO_2 and NO_x emissions from ships in North-East Atlantic waters: in situ measurements and comparison with an emission model, Environmental Science: Atmospheres, https://doi.org/10.1039/D5EA00089K, 2025.

Lee, Y. H., Adams, P. J., and Shindell, D. T.: Evaluation of the global aerosol microphysical ModelE2-TOMAS model against satellite and ground-based observations, Geoscientific Model Development, 8, 631–667, https://doi.org/10.5194/gmd-8-631-2015, 2015.

https://doi.org/10.5194/egusphere-2026-2654
Preprint. Discussion started: 20 May 2026

Lin, H. and Leaitch, W. R.: Development of an in-cloud aerosol activation parameterization for climate modelling, in: Proceedings of the WMO Workshop on Measurement of Cloud Properties for Forecasts of Weather, Air Quality and Climate, pp. 328–355, World Meteorological Organization, Mexico City, 1997.

Liu, X., Easter, R. C., Ghan, S. J., Zaveri, R., Rasch, P., Shi, X., Lamarque, J.-F., Gettelman, A., Morrison, H., Vitt, F., Conley, A., Park, S., Neale, R., Hannay, C., Ekman, A. M. L., Hess, P., Mahowald, N., Collins, W., Iacono, M. J., Bretherton, C. S., Flanner, M. G., and Mitchell, D.: Toward a minimal representation of aerosols in climate models: description and evaluation in the Community Atmosphere Model CAM5, Geoscientific Model Development, 5, 709–739, https://doi.org/10.5194/gmd-5-709-2012, 2012.

Loeb, N. G., Doelling, D. R., Wang, H., Su, W., Nguyen, C., Corbett, J. G., Liang, L., Mitrescu, C., Rose, F. G., and Kato, S.: Clouds and the Earth's Radiant Energy System (CERES) Energy Balanced and Filled (EBAF) Top-of-Atmosphere (TOA) Edition-4.0 data product, Journal of Climate, 31, 895–918, https://doi.org/10.1175/JCLI-D-17-0208.1, 2018.

Malavelle, F. F., Haywood, J. M., Jones, A., Gettelman, A., Clarisse, L., Bauduin, S., Allan, R. P., Karset, I. H. H., Kristjánsson, J. E., Oreopoulos, L., Cho, N., Lee, D., Bellouin, N., Boucher, O., Grosvenor, D. P., Carslaw, K. S., Dhomse, S., Mann, G. W., Schmidt, A., Coe, H., Hartley, M. E., Dalvi, M., Hill, A. A., Johnson, B. T., Johnson, C. E., Knight, J. R., O'Connor, F. M., Partridge, D. G., Stier, P., Myhre, G., Platnick, S., Stephens, G. L., Takahashi, H., and Thordarson, T.: Strong constraints on aerosol–cloud interactions from volcanic eruptions, Nature, 546, 485–491, https://doi.org/10.1038/nature22974, 2017.

Mann, G. W., Carslaw, K. S., Spracklen, D. V., Ridley, D. A., Manktelow, P. T., Chipperfield, M. P., Pickering, S. J., and Johnson, C. E.: Description and evaluation of GLOMAP-mode: a modal global aerosol microphysics model for the UKCA composition-climate model, Geoscientific Model Development, 3, 519–551, https://doi.org/10.5194/gmd-3-519-2010, 2010.

Mann, G. W., Carslaw, K. S., Ridley, D. A., Spracklen, D. V., et al.: Intercomparison of modal and sectional aerosol microphysics representations within the same 3-D global chemical transport model, Atmospheric Chemistry and Physics, 12, 4449–4476, https://doi.org/10.5194/acp-12-4449-2012, 2012.

Manshausen, P., Watson-Parris, D., Christensen, M. W., Jalkanen, J.-P., and Stier, P.: Rapid saturation of cloud water adjustments to shipping emissions, Atmospheric Chemistry and Physics, 23, 12 545–12 555, https://doi.org/10.5194/acp-23-12545-2023, 2023.

Mao, J., Zhang, Y., Yu, F., Nair, A. A., Yu, Q., Wang, L., Ma, W., and Chen, L.: On the Ship Particle Number Emission Index: Size-Resolved Microphysics and Key Controlling Parameters, Journal of Geophysical Research: Atmospheres, 126, e2020JD034 427, https://doi.org/10.1029/2020JD034427, 2021.

March, D., Metcalfe, K., Tintoré, J., and Godley, B. J.: Tracking the global reduction of marine traffic during the COVID-19 pandemic, Nature Communications, 12, 2415, https://doi.org/10.1038/s41467-021-22423-6, 2021.

McDuffie, E. E., Smith, S. J., O'Rourke, P., Tibrewal, K., Venkataraman, C., Marais, E. A., Zheng, B., Crippa, M., Brauer, M., and Martin, R. V.: A global anthropogenic emission inventory of atmospheric pollutants from sector- and fuel-specific sources (1970–2017): an application of the Community Emissions Data System (CEDS), Earth System Science Data, 12, 3413–3442, https://doi.org/10.5194/essd-12-3413-2020, 2020.

Menon, S. and Rotstayn, L.: The radiative influence of aerosol effects on liquid-phase cumulus and stratiform clouds based on sensitivity studies with two climate models, Climate Dynamics, 27, 345–356, https://doi.org/10.1007/s00382-006-0139-3, 2006.

Morcrette, C. J.: Improvements to a prognostic cloud scheme through changes to its cloud erosion parametrization, Atmospheric Science Letters, 13, 95–102, https://doi.org/10.1002/asl.374, 2012.

Mueller, N., Westerby, M., and Nieuwenhuijsen, M.: Health impact assessments of shipping and port-sourced air pollution on a global scale: A scoping literature review, Environmental Research, 216, 114 460, https://doi.org/10.1016/j.envres.2022.114460, 2023.

https://doi.org/10.5194/egusphere-2026-2654
Preprint. Discussion started: 20 May 2026

Mulcahy, J. P., Jones, C. G., Rumbold, S. T., Kuhlbrodt, T., Dittus, A. J., Blockley, E. W., Yool, A., Walton, J., Hardacre, C., Andrews, T., Bodas-Salcedo, A., Stringer, M., De Mora, L., Harris, P., Hill, R., Kelley, D., Robertson, E., and Tang, Y.: UKESM1.1: development and evaluation of an updated configuration of the UK Earth System Model, Geoscientific Model Development, 16, 1569–1600, https://doi.org/10.5194/gmd-16-1569-2023, 2023.

Mülmenstädt, J., Ackerman, A. S., Fridlind, A. M., Huang, M., Ma, P.-L., Mahfouz, N., Bauer, S. E., Burrows, S. M., Christensen, M. W., Dipu, S., Gettelman, A., Leung, L. R., Tornow, F., Quaas, J., Varble, A. C., Wang, H., Zhang, K., and Zheng, Y.: Can general circulation models (GCMs) represent cloud liquid water path adjustments to aerosol–cloud interactions?, Atmospheric Chemistry and Physics, 24, 13 633–13 652, https://doi.org/10.5194/acp-24-13633-2024, 2024a.

Mülmenstädt, J., Gryspeerdt, E., Dipu, S., Quaas, J., Ackerman, A. S., Fridlind, A. M., Tornow, F., Bauer, S. E., Gettelman, A., Ming, Y., Zheng, Y., Ma, P.-L., Wang, H., Zhang, K., Christensen, M. W., Varble, A. C., Leung, L. R., Liu, X., Neubauer, D., Partridge, D. G., Stier, P., and Takemura, T.: General circulation models simulate negative liquid water path–droplet number correlations, but anthropogenic aerosols still increase simulated liquid water path, Atmospheric Chemistry and Physics, 24, 7331–7345, https://doi.org/10.5194/acp-24-7331-2024, 2024b.

Nenes, A. and Seinfeld, J. H.: Parameterization of cloud droplet formation in global climate models, Journal of Geophysical Research: Atmospheres, 108, https://doi.org/10.1029/2002JD002911, 2003.

O'Neill, B. C., Tebaldi, C., van Vuuren, D. P., Eyring, V., Friedlingstein, P., Hurtt, G., Knutti, R., Kriegler, E., Lamarque, J.-F., Lowe, J., Meehl, G. A., Moss, R., Riahi, K., and Sanderson, B. M.: The Scenario Model Intercomparison Project (ScenarioMIP) for CMIP6, Geoscientific Model Development, 9, 3461–3482, https://doi.org/10.5194/gmd-9-3461-2016, 2016.

Partanen, A. I., Laakso, A., Schmidt, A., Kokkola, H., Kuokkanen, T., Pietikäinen, J.-P., Kerminen, V.-M., Lehtinen, K. E. J., Laakso, L., and Korhonen, H.: Climate and air quality trade-offs in altering ship fuel sulfur content, Atmospheric Chemistry and Physics, 13, 12 059–12 071, https://doi.org/10.5194/acp-13-12059-2013, 2013.

Peters, K., Stier, P., Quaas, J., and Graßl, H.: Aerosol indirect effects from shipping emissions: sensitivity studies with the global aerosol-climate model ECHAM-HAM, Atmospheric Chemistry and Physics, 12, 5985–6007, https://doi.org/10.5194/acp-12-5985-2012, 2012.

Peters, K., Stier, P., Quaas, J., and Graßl, H.: Corrigendum to "Aerosol indirect effects from shipping emissions: sensitivity studies with the global aerosol-climate model ECHAM-HAM" published in Atmos. Chem. Phys., 12, 5985–6007, 2012, Atmospheric Chemistry and Physics, 13, 6429–6430, https://doi.org/10.5194/acp-13-6429-2013, 2013.

Petters, M. D. and Kreidenweis, S. M.: A single parameter representation of hygroscopic growth and cloud condensation nucleus activity, Atmospheric Chemistry and Physics, 7, 1961–1971, https://doi.org/10.5194/acp-7-1961-2007, 2007.

Petzold, A., Hasselbach, J., Lauer, P., Baumann, R., Franke, K., Gurk, C., Schlager, H., and Weingartner, E.: Experimental studies on particle emissions from cruising ship, their characteristic properties, transformation and atmospheric lifetime in the marine boundary layer, Atmospheric Chemistry and Physics, 8, 2387–2403, https://doi.org/10.5194/acp-8-2387-2008, 2008.

Phinney, L. A., Lohmann, U., and Leaitch, W. R.: Limitations of using an equilibrium approximation in an aerosol activation parameterization, Journal of Geophysical Research: Atmospheres, 108, 2002JD002 391, https://doi.org/10.1029/2002JD002391, 2003.

Possner, A., Zubler, E., Lohmann, U., and Schär, C.: The resolution dependence of cloud effects and ship-induced aerosol-cloud interactions in marine stratocumulus, Journal of Geophysical Research: Atmospheres, 121, 4810–4829, https://doi.org/10.1002/2015JD024685, 2016.

Quaglia, I. and Visioni, D.: Modeling 2020 regulatory changes in international shipping emissions helps explain anomalous 2023 warming, Earth System Dynamics, 15, 1527–1541, https://doi.org/10.5194/esd-15-1527-2024, 2024.

https://doi.org/10.5194/egusphere-2026-2654
Preprint. Discussion started: 20 May 2026

Reutter, P., Su, H., Trentmann, J., Simmel, M., Rose, D., Gunthe, S. S., Wernli, H., Andreae, M. O., and Pöschl, U.: Aerosol- and updraft-limited regimes of cloud droplet formation: influence of particle number, size and hygroscopicity on the activation of cloud condensation nuclei (CCN), Atmospheric Chemistry and Physics, 9, 7067–7080, https://doi.org/10.5194/acp-9-7067-2009, 2009.

Righi, M., Klinger, C., Eyring, V., Hendricks, J., Lauer, A., and Petzold, A.: Climate Impact of Biofuels in Shipping: Global Model Studies of the Aerosol Indirect Effect, Environmental Science & Technology, 45, 3519–3525, https://doi.org/10.1021/es1036157, 2011.

Seland, Ø., Bentsen, M., Olivié, D., Toniazzo, T., Gjermundsen, A., Graff, L. S., Debernard, J. B., Gupta, A. K., He, Y.-C., Kirkevåg, A., Schwinger, J., Tjiputra, J., Aas, K. S., Bethke, I., Fan, Y., Griesfeller, J., Grini, A., Guo, C., Ilicak, M., Karset, I. H. H., Landgren, O., Liakka, J., Moseid, K. O., Nummelin, A., Spensberger, C., Tang, H., Zhang, Z., Heinze, C., Iversen, T., and Schulz, M.: Overview of the Norwegian Earth System Model (NorESM2) and key climate response of CMIP6 DECK, historical, and scenario simulations, Geoscientific Model Development, 13, 6165–6200, https://doi.org/10.5194/gmd-13-6165-2020, 2020.

Skeie, R. B., Byrom, R., Hodnebrog, Ø., Jouan, C., and Myhre, G.: Multi-model effective radiative forcing of the 2020 sulfur cap for shipping, Atmospheric Chemistry and Physics, 24, 13 361–13 370, https://doi.org/10.5194/acp-24-13361-2024, 2024.

Small, J. D., Chuang, P. Y., Feingold, G., and Jiang, H.: Can aerosol decrease cloud lifetime?, Geophysical Research Letters, 36, https://doi.org/10.1029/2009GL038888, 2009.

Smith, J.: Data and Code in Support of: Recent Modelling Studies Systematically Underestimate the Warming from IMO2020 Shipping Regulations, https://doi.org/10.5281/zenodo.20076408, dataset, 2026.

Sofiev, M., Winebrake, J. J., Johansson, L., Carr, E. W., Prank, M., Soares, J., Vira, J., Kouznetsov, R., Jalkanen, J.-P., and Corbett, J. J.: Cleaner fuels for ships provide public health benefits with climate tradeoffs, Nature Communications, 9, 406, https://doi.org/10.1038/s41467-017-02774-9, 2018.

Stevens, B. and Feingold, G.: Untangling aerosol effects on clouds and precipitation in a buffered system, Nature, 461, 607–613, https://doi.org/10.1038/nature08281, 2009.

Stevens, R. G., Pierce, J. R., Brock, C. A., Reed, M. K., Crawford, J. H., Holloway, J. S., Ryerson, T. B., Huey, L. G., and Nowak, J. B.: Nucleation and growth of sulfate aerosol in coal-fired power plant plumes: sensitivity to background aerosol and meteorology, Atmospheric Chemistry and Physics, 12, 189–206, https://doi.org/10.5194/acp-12-189-2012, 2012.

Stier, P., Feichter, J., Kinne, S., Kloster, S., Vignati, E., Wilson, J., Ganzeveld, L., Tegen, I., Werner, M., Balkanski, Y., Schulz, M., Boucher, O., Minikin, A., and Petzold, A.: The aerosol-climate model ECHAM5-HAM, Atmospheric Chemistry and Physics, 5, 1125–1156, https://doi.org/10.5194/acp-5-1125-2005, 2005.

Tegen, I., Neubauer, D., Ferrachat, S., Siegenthaler-Le Drian, C., Bey, I., Schutgens, N., Stier, P., Watson-Parris, D., Stanelle, T., Schmidt, H., Rast, S., Kokkola, H., Schultz, M., Schroeder, S., Daskalakis, N., Barthel, S., Heinold, B., and Lohmann, U.: The global aerosol–climate model ECHAM6.3–HAM2.3 – Part 1: Aerosol evaluation, Geoscientific Model Development, 12, 1643–1677, https://doi.org/10.5194/gmd-12-1643-2019, 2019.

Tian, J., Riemer, N., West, M., Pfaffenberger, L., Schlager, H., and Petzold, A.: Modeling the evolution of aerosol particles in a ship plume using PartMC-MOSAIC, Atmospheric Chemistry and Physics, 14, 5327–5347, https://doi.org/10.5194/acp-14-5327-2014, 2014.

Tilmes, S., Lamarque, J.-F., Emmons, L. K., Kinnison, D. E., Ma, P.-L., Liu, X., Ghan, S., Bardeen, C., Arnold, S., Deeter, M., Vitt, F., Ryerson, T., Elkins, J. W., Moore, F., Spackman, J. R., and Val Martin, M.: Description and evaluation of tropospheric chemistry and aerosols in the Community Earth System Model (CESM1.2), Geoscientific Model Development, 8, 1395–1426, https://doi.org/10.5194/gmd-8-1395-2015, 2015.

https://doi.org/10.5194/egusphere-2026-2654
Preprint. Discussion started: 20 May 2026

Twohy, C. H., Petters, M. D., Snider, J. R., Stevens, B., Tahnk, W., Wetzel, M., Russell, L., and Burnet, F.: Evaluation of the aerosol indirect effect in marine stratocumulus clouds: Droplet number, size, liquid water path, and radiative impact, Journal of Geophysical Research: Atmospheres, 110, 2004JD005 116, https://doi.org/10.1029/2004JD005116, 2005.

Twomey, S.: Pollution and the planetary albedo, Atmospheric Environment, 8, 1251–1256, 1974.

Twomey, S.: The influence of pollution on the shortwave albedo of clouds, Journal of the Atmospheric Sciences, 34, 1149–1152, 1977.

Virtanen, A., Joutsensaari, J., Kokkola, H., Partridge, D. G., Blichner, S., Seland, Ø., Holopainen, E., Tovazzi, E., Lipponen, A., Mikkonen, S., Leskinen, A., Hyvärinen, A.-P., Zieger, P., Krejci, R., Ekman, A. M. L., Riipinen, I., Quaas, J., and Romakkaniemi, S.: High sensitivity of cloud formation to aerosol changes, Nature Geoscience, 18, 289–295, https://doi.org/10.1038/s41561-025-01662-y, 2025.

Walters, D., Baran, A. J., Boutle, I., et al.: The Met Office Unified Model Global Atmosphere 7.0/7.1 and JULES Global Land 7.0 configurations, Geoscientific Model Development, 12, 1909–1963, https://doi.org/10.5194/gmd-12-1909-2019, 2019.

Watson-Parris, D., Christensen, M. W., Laurenson, A., Clewley, D., Gryspeerdt, E., and Stier, P.: Shipping regulations lead to large reduction in cloud perturbations, Proceedings of the National Academy of Sciences, 119, e2206885 119, https://doi.org/10.1073/pnas.2206885119, 2022.

Watson-Parris, D., Wilcox, L. J., Stjern, C. W., Allen, R. J., Persad, G., Bollasina, M. A., Ekman, A. M. L., Iles, C. E., Joshi, M., Lund, M. T., McCoy, D., Westervelt, D. M., Williams, A. I. L., and Samset, B. H.: Surface temperature effects of recent reductions in shipping SO_2 emissions are within internal variability, Atmospheric Chemistry and Physics, 25, 4443–4454, https://doi.org/10.5194/acp-25-4443-2025, 2025.

West, R. E. L., Stier, P., Jones, A., Johnson, C. E., Mann, G. W., Bellouin, N., Partridge, D. G., and Kipling, Z.: The importance of vertical velocity variability for estimates of the indirect aerosol effects, Atmospheric Chemistry and Physics, 14, 6369–6393, https://doi.org/10.5194/acp-14-6369-2014, 2014.

Wilks, D. S.: On "field significance" and the false discovery rate, Journal of Applied Meteorology and Climatology, 45, 1181–1189, https://doi.org/10.1175/JAM2404.1, 2006.

Wilks, D. S.: "The stippling shows statistically significant grid points": How research results are routinely overstated and overinterpreted, and what to do about it, Bulletin of the American Meteorological Society, 97, 2263–2273, https://doi.org/10.1175/BAMS-D-15-00267.1, 2016.

Wilson, D. R. and Ballard, S. P.: A microphysically based precipitation scheme for the UK Meteorological Office Unified Model, Quarterly Journal of the Royal Meteorological Society, 125, 1607–1636, https://doi.org/10.1002/qj.49712555707, 1999.

Wilson, D. R., Bushell, A. C., Sherwood, S. C., et al.: PC2: A prognostic cloud fraction and condensation scheme. I: Scheme description, Quarterly Journal of the Royal Meteorological Society, 134, 2093–2107, https://doi.org/10.1002/qj.333, 2008.

Wood, R.: Stratocumulus Clouds, Monthly Weather Review, 140, 2373–2423, https://doi.org/10.1175/MWR-D-11-00121.1, 2012.

Woodward, S.: Modeling the atmospheric life cycle and radiative impact of mineral dust in the Hadley Centre climate model, Journal of Geophysical Research: Atmospheres, 106, 18 155–18 166, https://doi.org/10.1029/2000JD900795, 2001.

Xu, Y., Yu, Q., Zhang, Y., and Ma, W.: Numerical Study on the Plume Behavior of Multiple Stacks of Container Ships, Atmosphere, 12, 600, https://doi.org/10.3390/atmos12050600, 2021.

Yoshioka, M., Grosvenor, D. P., Booth, B. B. B., Morice, C. P., and Carslaw, K. S.: Warming effects of reduced sulfur emissions from shipping, Atmospheric Chemistry and Physics, 24, 13 681–13 692, https://doi.org/10.5194/acp-24-13681-2024, 2024.

https://doi.org/10.5194/egusphere-2026-2654
Preprint. Discussion started: 20 May 2026

Yu, C., Pasternak, D., Lee, J., Yang, M., Bell, T., Bower, K., Wu, H., Liu, D., Reed, C., Bauguitte, S., Cliff, S., Trembath, J., Coe, H., and Allan, J. D.: Characterizing the Particle Composition and Cloud Condensation Nuclei from Shipping Emission in Western Europe, Environmental Science & Technology, 54, 15 604–15 612, https://doi.org/10.1021/acs.est.0c04039, 2020.

Yuan, T., Song, H., Wood, R., Wang, C., Oreopoulos, L., Platnick, S. E., Von Hippel, S., Meyer, K., Light, S., and Wilcox, E.: Global reduction in ship-tracks from sulfur regulations for shipping fuel, Science Advances, 8, eabn7988, https://doi.org/10.1126/sciadv.abn7988, 2022.

Yuan, T., Song, H., Oreopoulos, L., Wood, R., Bian, H., Breen, K., Chin, M., Yu, H., Barahona, D., Meyer, K., and Platnick, S.: Observational evidence of strong forcing from aerosol effect on low cloud coverage, Science Advances, 9, eadh7716, https://doi.org/10.1126/sciadv.adh7716, 2023.

Yuan, T., Song, H., Oreopoulos, L., Wood, R., Bian, H., Breen, K., Chin, M., Yu, H., Barahona, D., Meyer, K., and Platnick, S.: Abrupt reduction in shipping emission as an inadvertent geoengineering termination shock produces substantial radiative warming, Communications Earth & Environment, 5, https://doi.org/10.1038/s43247-024-01442-3, 2024.

Zhang, J., Chen, Y.-S., Gryspeerdt, E., Yamaguchi, T., and Feingold, G.: Radiative forcing from the 2020 shipping fuel regulation is large but hard to detect, Communications Earth & Environment, 6, https://doi.org/10.1038/s43247-024-01911-9, 2025.

Zhang, K., O'Donnell, D., Kazil, J., Stier, P., Kinne, S., Lohmann, U., Ferrachat, S., Croft, B., Quaas, J., Wan, H., Rast, S., and Feichter, J.: The global aerosol-climate model ECHAM-HAM, version 2: sensitivity to improvements in process representations, Atmospheric Chemistry and Physics, 12, 8911–8949, https://doi.org/10.5194/acp-12-8911-2012, 2012.